



## **New Specimens of Microraptor zhaoianus (Theropoda: Dromaeosauridae) from Northeastern China**

Authors: HWANG, SUNNY H., NORELL, MARK A., QIANG, JI, and KEQIN, GAO

Source: American Museum Novitates, 2002(3381) : 1-44

Published By: American Museum of Natural History

URL: [https://doi.org/10.1206/0003-0082\(2002\)381<0001:NSOMZT>2.0.CO;2](https://doi.org/10.1206/0003-0082(2002)381<0001:NSOMZT>2.0.CO;2)

---

BioOne Complete (complete.BioOne.org) is a full-text database of 200 subscribed and open-access titles in the biological, ecological, and environmental sciences published by nonprofit societies, associations, museums, institutions, and presses.

Your use of this PDF, the BioOne Complete website, and all posted and associated content indicates your acceptance of BioOne's Terms of Use, available at [www.bioone.org/terms-of-use](http://www.bioone.org/terms-of-use).

Usage of BioOne Complete content is strictly limited to personal, educational, and non - commercial use. Commercial inquiries or rights and permissions requests should be directed to the individual publisher as copyright holder.

---

BioOne sees sustainable scholarly publishing as an inherently collaborative enterprise connecting authors, nonprofit publishers, academic institutions, research libraries, and research funders in the common goal of maximizing access to critical research.

# AMERICAN MUSEUM *Novitates*

PUBLISHED BY THE AMERICAN MUSEUM OF NATURAL HISTORY  
CENTRAL PARK WEST AT 79TH STREET, NEW YORK, NY 10024

Number 3381, 44 pp., 31 figures, 2 tables

August 16, 2002

## New Specimens of *Microraptor zhaoianus* (Theropoda: Dromaeosauridae) from Northeastern China

SUNNY H. HWANG,<sup>1</sup> MARK A. NORELL,<sup>2</sup> JI QIANG,<sup>3</sup> AND GAO KEQIN<sup>4</sup>

### ABSTRACT

New specimens of the diminutive theropod dinosaur *Microraptor zhaoianus* are described. These specimens preserve significant morphological details that are not present or are poorly preserved in the holotype specimen, including aspects of the manus, pectoral girdle, dorsal vertebrae, ilium, and sacrum. These specimens were coded into a current matrix of theropod morphological characters. *Microraptor* is found to be the sister taxon to other dromaeosaurs. Dromaeosaurids are monophyletic and together with a monophyletic troodontid group form a monophyletic Deinonychosauria, which is the sister taxon to Avialae. Apparently small size is primitive for Deinonychosauria, which has implications for bird origins.

### INTRODUCTION

Recently, Xu et al. (2000) described the smallest known non-avian theropod *Microraptor zhaoianus*. This description was based on an incomplete specimen, Institute of Vertebrate Paleontology and Paleoanthropology (IVPP) V12330, from the early Cretaceous

rocks of Liaoning Province, China. This animal is exciting both because it is so small (about 55 cm long as an adult) and because of its phylogenetic position near the base of the Dromaeosauridae (Xu et al., 2000), a clade that is considered by many to have close affinities with avialans (Gauthier, 1986; Sereno, 1999; Norell et al., 2001). While di-

<sup>1</sup> Graduate Student, Division of Paleontology, American Museum of Natural History. e-mail: sunny@amnh.org

<sup>2</sup> Chairman, Division of Paleontology, American Museum of Natural History. e-mail: norell@amnh.org

<sup>3</sup> Professor, Chinese Academy of Geological Sciences. 26 Baiwanzhuang, Beijing 100037, People's Republic of China.

<sup>4</sup> Professor, Department of Geology, Peking University, Beijing 100871, People's Republic of China; Research Associate, Division of Paleontology, American Museum of Natural History.



Fig. 1. Map of Liaoning Province showing the collection site of CAGS 20-7-004 and CAGS 20-8-001.

agnostic, the holotype lacks many important parts of the skeleton, including most of the manus, pectoral girdle, and dorsal vertebrae. Additionally, most of the ilium, the sacrum, and the dorsal and cervical vertebrae were either poorly preserved or not visible. Here we provide descriptions of two additional specimens of *Microraptor zhaoianus* that provide new skeletal data for this important taxon.

The specimen slabs were collected by farmers from Qianyang—a small village approximately 10 km southwest of the city of Yixian in Liaoning Province, China (fig. 1). The specimens are housed in the collection of the Chinese Academy of Geological Sciences (CAGS). Unfortunately, CAGS 20-7-004 was poorly prepared and covered with low grade shellac before it was acquired by the CAGS (fig. 2). CAGS 20-8-001 is much better preserved, although much of the skeleton is missing (fig. 3).

These specimens can be confidently referred to *Microraptor zhaoianus* based on a number of diagnostic characters (Xu et al., 2000). CAGS 20-7-004 has teeth that are serrated only on the posterior carinae and constricted between the crown and root and long



Fig. 2. *Microraptor zhaoianus*, specimen CAGS 20-7-004. View of entire mounted slab.

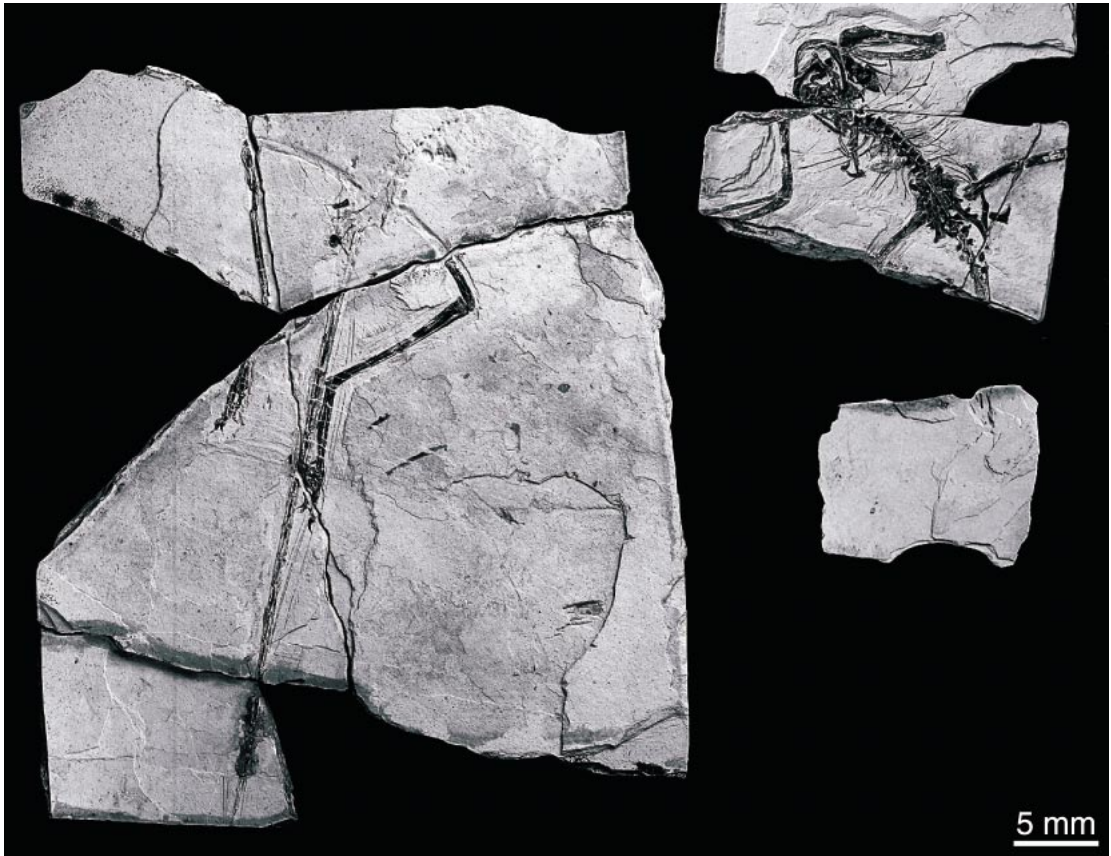


Fig. 3. *Microraptor zhaoianus*, specimen CAGS 20-8-001. View of all slabs and counterpart elements.

midcaudal vertebrae that are three to four times the length of the anterodorsal vertebrae (Xu et al., 2000). CAGS 20-7-004 also has large, strongly recurved pedal unguals with large flexor tubercles, a character considered by Xu et al. (2000) as diagnostic of *Microraptor zhaoianus*. However, such unguals occur in all dromaeosaurs where these features are adequately preserved. CAGS 20-8-001 displays an anterior accessory crest just distal to the lesser trochanter on the femur, and like CAGS 20-7-004 has long midcaudal vertebrae (Xu et al., 2000).

#### MATERIAL

CAGS 20-8-001 is made up of seven slabs, which have not all been split along the same planes (fig. 3). As a result, the dorsal surfaces of the pectoral girdle, forelimbs,

trunk, pelvic girdle, proximal femora, and proximal caudals are exposed, while the ventral surfaces of the distal femora, tibiae, fibulae, pes, and distal caudals are exposed. The counterslab is available only for the midsection of the body. Despite the multiple slabs on which the specimen is contained, it is well preserved and almost fully articulated.

CAGS 20-7-004 is preserved as a single slab mounted on a plaster block with a few counterpart pieces preserved. The specimen is semi-articulated; however, some elements like the lower jaws, lay near the edge of the slab. Relevant measurements are presented in appendix 1.

#### DESCRIPTION

##### SKULL

Identifiable cranial remains are only known for CAGS 20-7-004, and these are

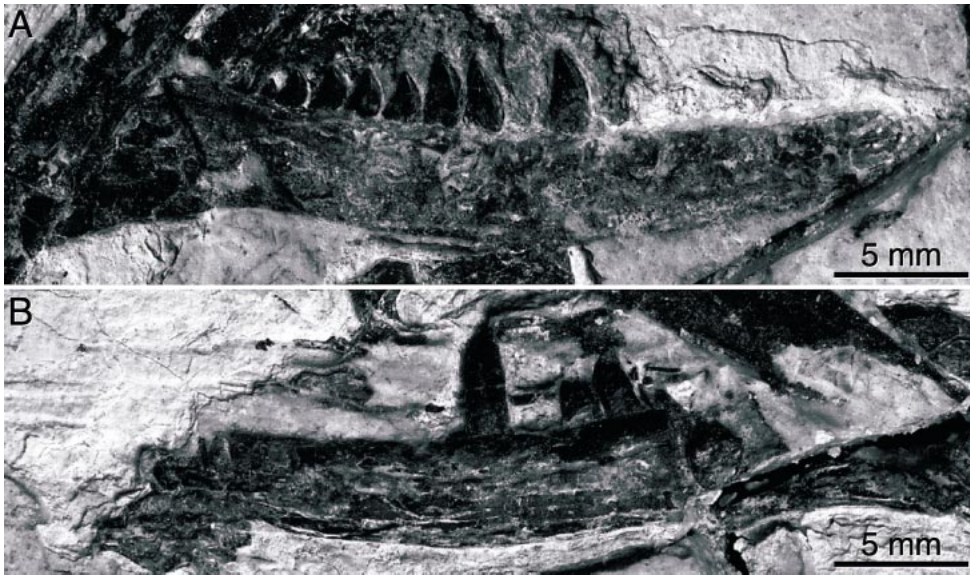


Fig. 4. (A) Right and (B) left dentaries of CAGS 20-7-004 in labial view.

limited to the two dentaries and splenials. The disarticulated dentaries lie in the slab with their labial surfaces exposed (fig. 4). The right dentary is complete, and has some surface breakage at its posterior end, but is otherwise well preserved. Only the posterior portion of the left dentary is preserved. In both dentaries, only posterior teeth are pre-

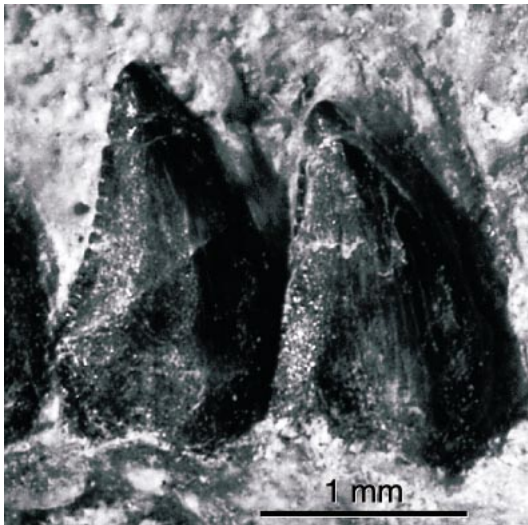


Fig. 5. Detail of posterior teeth of right dentary of CAGS 20-7-004.

served. These posterior teeth are very troodontid-like, as noted by Xu et al. (2000). The teeth have denticles only on their posterior carinae; these denticles are relatively large and point toward the tooth apices (fig. 5). There are approximately 8 denticles per millimeter, with an average basal denticle diameter of 0.1 mm, and a maximum basal denticle diameter of 0.12 mm. The denticles are not as sharply hooked or as triangular as those on the posterior carinae of some troodontid teeth; instead, they are more square and gently hooked, like those on the anterior carinae of some troodontid teeth (Currie, 1987). The teeth of *Microraptor* are also constricted between the crown and root, giving them the characteristic “waisted” appearance of troodontid teeth. Unfortunately, because none of the anterior teeth have been preserved, Xu et al.’s (2000) description of completely unserrated anterior teeth in IVPP V12330 cannot be confirmed. The dentition of *Microraptor* is especially similar to that of the basal troodontid *Sinovenator* (Xu et al., 2002), which also has unserrated anterior teeth, posterior teeth serrated only on the posterior carinae, and denticles similar in size to those of dromaeosaurids.

The teeth are closely packed, as in troodontids (Currie, 1987), and decrease in size

towards the back of the jaw (fig. 4). Eight of the last nine teeth are present in the right dentary; one tooth in the series is missing. Assuming that the posterior dentary teeth are about 150% wider than the anterior dentary teeth at the base of the crown (estimated from fig. 2 in Xu et al., 2000), there is room for approximately 10 more teeth in the anterior of the right dentary. This suggests a total of 19 teeth in each dentary, more than in any other dromaeosaurid (see Currie, 1995, for data and additional references).

The dentaries are long and shallow as in other dromaeosaurs (Norell and Makovicky, in press), but relatively thick labiolingually. The tooth row is noticeably inset from the lateral margin of the dentary, as in *Sinovenator* (Xu et al., 2002). As in other dromaeosaurids, the dorsal and ventral margins of the dentary are subparallel, tapering only slightly anteriorly (Currie, 1995). There are two rows of foramina on the labial surface of the dentary: one below the dorsal margin of the dental shelf and one just above the ventral border of the dentary. The upper row is composed of larger foramina. A posteroventrally extending flange drops from the posterior end of the dentary. The broken surface at the posterior of the right dentary reveals a foramen on the lingual side of the dentary, which is either part of the internal mandibular fenestra or the posterior widening of the Meckelian canal. The splenial is exposed on the lateral surface of the dentary as a long wedge caudal to the posteroventral corner of the dentary.

#### VERTEBRAE

Fifteen closely associated, or articulated, presacral vertebrae are preserved in CAGS 20-8-001. Assuming 13 dorsal vertebrae as in other dromaeosaurids (Ostrom, 1969; Norell and Makovicky, 1999), then two posterior cervical vertebrae are present, presumably the last two cervicals.

The two posterior cervicals are preserved in dorsal view (fig. 6). These vertebrae are X-shaped. The neural spine is short and centered on the neural arch. The vertebrae are anteroposteriorly short, and the centra do not extend past the anterior or posterior extent of the neural arch. The transverse processes are

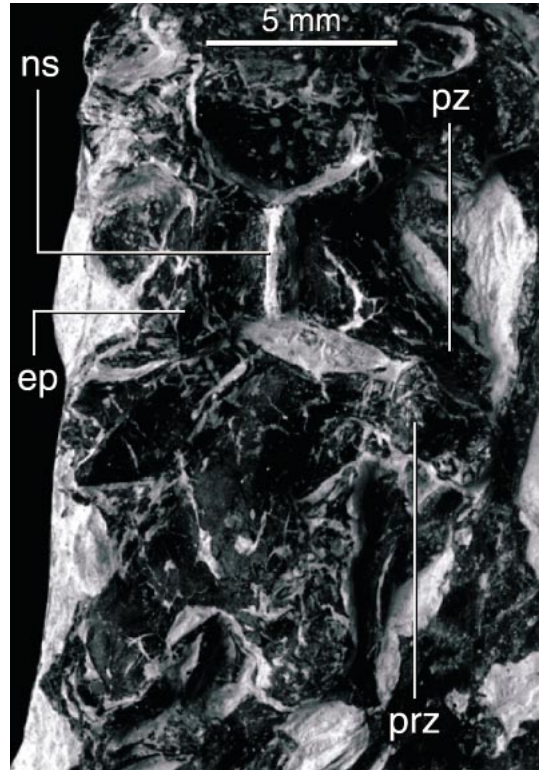


Fig. 6. Posterior cervical vertebrae of CAGS 20-8-001 in dorsal view. Anatomical labels for all figures are spelled out in appendix 3.

reduced and are positioned just anterior to the midpoint of the neural arch. The distal ends of the prezygapophyses flare transversely. The prezygapophyses spread widely from the midline and extend further laterally than the postzygapophyses. The postzygapophyses are small and subcircular; small epiphyses extend only to the midpoint of the dorsal postzygapophyseal surface.

One cervical vertebra is preserved in CAGS 20-7-004 (fig. 7). It is identifiable as the last cervical vertebra because it is in articulation with the first dorsal vertebra. The left transverse process and zygapophyses are fragmented, but the centrum is well preserved, and the right apophyses are intact but shifted posteriorly. The ventral surface of this vertebra is exposed, revealing a centrum wider at its anterior than at its posterior. The posterior end of the centrum extends more ventrally than the anterior, so that it is triangular in lateral view. The anterior inter-

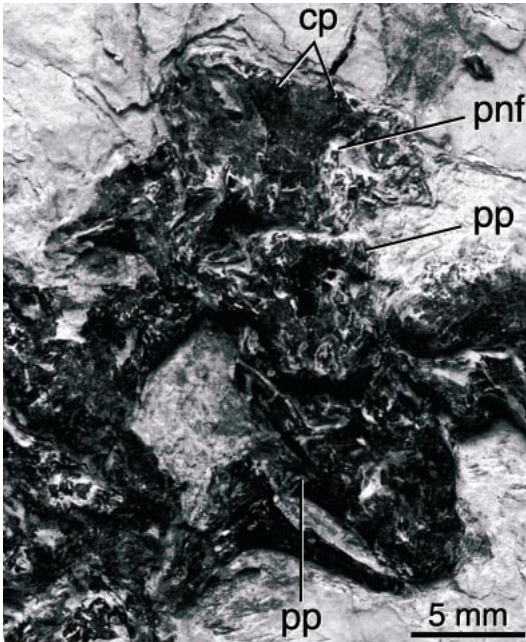


Fig. 7. Cervico-dorsal transition in CAGS 20-7-004. Last cervical vertebra in ventral view, first dorsal in ventral view, and second dorsal in anterior view.

vertebral articulation is angled posteroventrally from its dorsal margin, as in other dromaeosaurids, and the posterior intervertebral articulation is more or less vertical. The parapophyses are located on the ventrolateral corners of the anterior articulation. Two large, prominent carotid processes are located on the ventral surface of the centrum just medial to the parapophyses. A broad, shallow sulcus runs between the two carotid processes along the ventral length of the centrum. The transverse processes appear pneumatic, with one large fossa opening into each. The edge of the transverse process overhangs this fossa. On the uncrushed right side, a relatively thick bar of bone, which is probably one of the struts that supports the transverse process, can be seen extending dorsally to the posterolaterally directed postzygapophysis.

The probable first dorsal of CAGS 20-8-001 is covered for the most part by the preceding cervical, so all that can be seen is that it has small postzygapophyses and epiphyses identical to those of the preceding

cervical. No transverse processes are visible, indicating that this may be the last cervical, not the first dorsal. The area around the cervico-dorsal transition is crushed, so exact identifications are difficult. The next three dorsals are also crushed and lie at a junction between two slabs of the specimen. It can be seen that the transverse processes are large and pronounced, unlike in the cervicals, and that the neural spines are taller and longer.

CAGS 20-7-004 provides more information about the anterior dorsals. The first dorsal, which is articulated with the cervical described previously, is also embedded in the matrix with its ventral surface exposed (fig. 7). It is narrower in cross section than the cervical, and the centrum is constricted mid-length. The first dorsal has a ventral midline keel as in the anterior dorsals of other dromaeosaurids, but it is unusual in that no large hypapophysis is present on the anteroventral surface of the centrum (Makovicky, 1995). The parapophyses are very low on the centrum, positioned slightly ventral to mid-height. The second dorsal is in association with the first dorsal but is rotated with respect to the first dorsal so that it is visible in anterior view (fig. 7). The transverse processes and prezygapophyses are missing. Its anterior intervertebral articulation is subtriangular, and it also does not have a large hypapophysis. Xu et al. (2000) coded hypapophyses as present in the holotype, and all other dromaeosaurs have hypapophyses of varying morphology (Norell and Makovicky, in press). Consequently, the absence of hypapophyses in CAGS 20-7-004 may be due to the poor preservation of the specimen. The prominent parapophyses, which have capitular articulations set on robust stalks, are in contact with the neural arch but still partly on the centrum, which confirms that this vertebra is the second dorsal (Makovicky, 1995).

The last nine dorsals (presumably the 5th through the 13th) of CAGS 20-8-001 are articulated and extremely well preserved in lateral view (fig. 8). There are no hypapophyses present on the anterior dorsals in the articulated series, but hypapophyses are not expected beyond the fourth dorsal. The transverse processes of the fifth, sixth, and seventh dorsals slant posterodorsally, whereas

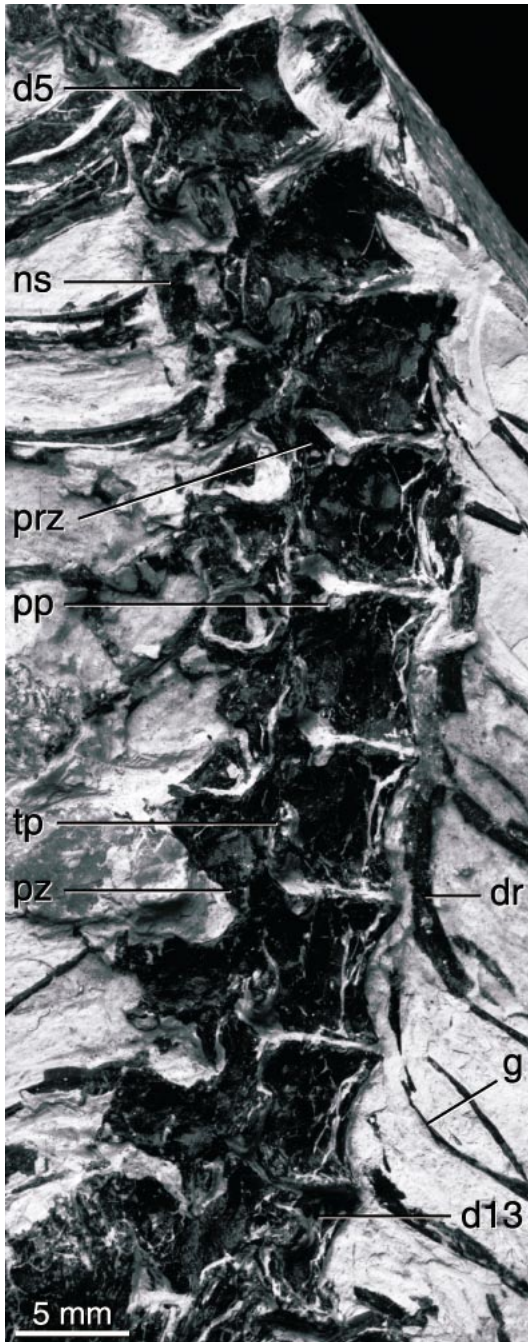


Fig. 8. Articated dorsal series of CAGS 20-8-001 in right lateral view.

those on the remaining dorsals, while still directed posteriorly, are more or less horizontal. The transverse processes also become shorter posteriorly along the series. Unlike *Velociraptor mongoliensis* (Norell and Makovicky, 1999) and *Deinonychus antirrhopus* (Ostrom, 1969), there are no pneumatic foramina present on any of the articulated dorsals, neither on the centra nor invading the transverse processes. Dorsals 8 through 13 of CAGS 20-7-004, which are split longitudinally and preserved on slab and counterslab, confirm that the centra of the posterior dorsals are solid, with no pneumatic divisions. The small parapophyses are set on short stalks as is typical for dromaeosaurids (Norell and Makovicky, 1999, in press) and are located on the neural arch, level with the bases of the prezygapophyseal hypantra. The position of the parapophyses does not change throughout the series. The centra are elongated relative to those of other dromaeosaurids, being approximately twice as long as they are tall. As a result, the neural spines of these dorsals are also relatively elongate, being square rather than bladelike as in other dromaeosaurids. This feature was not noted by Xu et al. (2000), but it is diagnostic of *Microraptor zhaoianus*. Neural spine height increases slightly posteriorly along the series. The distal or dorsal surfaces of the neural spines are not expanded for the insertion of the interspinous ligament as has been observed in *Velociraptor mongoliensis* (Norell and Makovicky, 1999), but are straight (flat) as in other dromaeosaurs. The anterior and posterior faces of the dorsals have a rugose rim. The ventral surfaces of the dorsals are uniformly concave throughout the series. The neural arches are completely fused to the centra. The prezygapophyses have well-developed hypantra; due to the articulation of the dorsals and their orientation with only the lateral surfaces exposed, the development of the postzygapophyseal hyposphenes cannot be determined. The zygapophyses of each dorsal are short, barely overlapping the centra of the preceding and succeeding vertebrae. In CAGS 20-7-004, the fourth through seventh dorsal vertebrae are exposed in dorsal view and show a slight variation in their zygapophyses. The anteriormost vertebra in the series, the fourth dorsal, has subcircular





Fig. 9. Sacrum of CAGS 20-8-001 in dorsal view.

pre- and postzygapophyses that are directed slightly anterolaterally and posterolaterally, respectively. By the seventh dorsal, the zygapophyses have become slightly more elongate and square, and are parallel to each other. The last dorsal was probably not fused to the sacrum, as it is disarticulated from the

first sacral vertebra in CAGS 20-8-001 and is still articulated to the 12th dorsal (fig. 8).

The sacrum is preserved in dorsal view on the slab on CAGS 20-8-001 (fig. 9). The preacetabular blades of the ilium cover the anterior sacrals, but judging from the length of the visible sacrals, there are either five or

six sacral vertebrae as in other adult dromaeosaurs (Norell and Makovicky, in press). The neural spines of the anterior sacrals are coossified into a thin continuous lamina running longitudinally along the midline of the sacrum. The posterior half of the neural spine of the last sacral is broken, but the lamina continues onto the anterior half of the last sacral, suggesting that the neural spine of the last sacral was fused to those of the others. Where the dorsal edges of the ilia have been broken away, the fusion of the transverse processes of the last two sacrals to the ilia is evident (fig. 9). The transverse processes are broadly expanded distally; the anteroposterior distal length of the last pair of transverse processes is equal to the longitudinal length of the last sacral vertebra. The zygapophyses of the sacral vertebrae are fused but do not form as prominent a ridge as seen in *Velociraptor mongoliensis* (Norell and Makovicky, 1997). The extent of fusion between the sacral centra is unknown due to the orientation of the sacrum in the slab, but it is probably extensive, based on the extent of fusion visible in other parts of the sacrum.

The entire articulated tail, which is wrapped in the extremely long, bony, rodlike extensions of the prezygapophyses and chevrons typical of dromaeosaurids, is present in CAGS 20-8-001; unfortunately, it is preserved on five different slabs, and segments have been lost and contacts between the slabs are not confluent (fig. 10A, B). The entire tail of CAGS 20-7-004 is also preserved, but the first three caudals are disarticulated from the rest of the rod-bound tail and scattered nearby (fig. 10C). Xu et al. (2000) counted 24 or 25 caudal vertebrae in the holotype and considered a tail with fewer than 26 vertebrae to be a diagnostic character of *Microraptor*, but there are approximately 26 caudal vertebrae in both CAGS 20-7-004 and CAGS 20-8-001. If Xu et al.'s (2000) count is correct, then *Microraptor* shows the same one or two vertebra (e) variation in caudal length seen in different specimens of *Archaeopteryx lithographica* (Wellnhofer, 1974, 1992, 1993).

In CAGS 20-8-001, the first caudal vertebra appears to be incompletely fused to the last sacral, but its transverse processes do not articulate with the ilia (figs. 9, 11). The anterior caudals are short, with broad transverse



Fig. 10. Tails of the *Microraptor* specimens. (A) Anterior caudal vertebrae of CAGS 20-8-001 on slab. (B) Remainder of caudal vertebrae of CAGS 20-8-001 on counterslab. (C) Caudal vertebrae of CAGS 20-7-004. Note the rodlike extensions of the prezygapophyses and chevrons that surround and stiffen both tails.

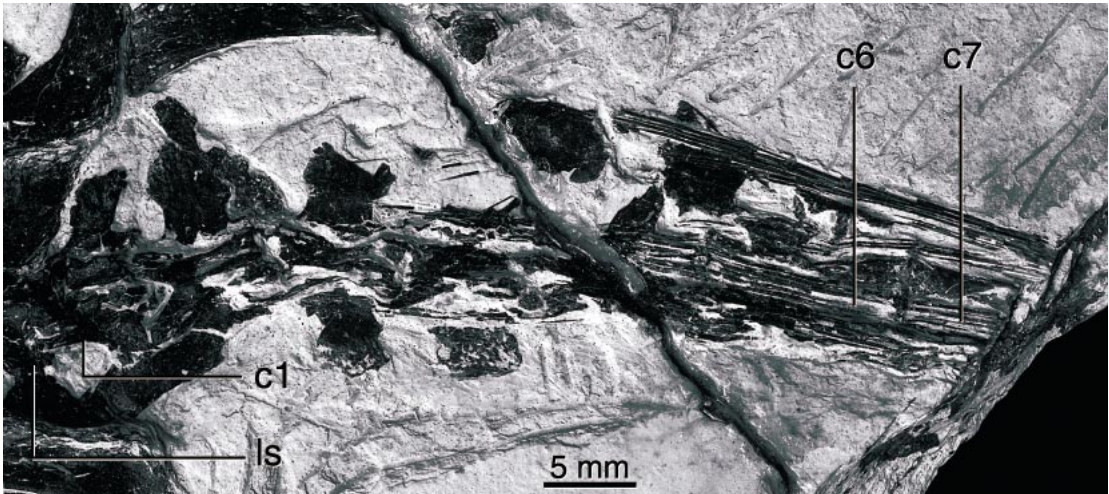


Fig. 11. Anterior caudal vertebrae of CAGS 20-8-001 in dorsal view.

processes that point posteriorly and neural spines that span the entire length of the neural arch (the height of the spines is indeterminate, as their distal ends are embedded in the counterslab). The prezygapophyses are approximately three times as long as the short postzygapophyses and overlap about one-third of the preceding vertebra. The prezygapophyses diverge laterally from the midpoint of the vertebrae, while the postzygapophyses are subparallel. The postzygapophyses taper to a blunt point posteriorly. The first two caudals in CAGS 20-7-004 are also visible in dorsal view, and they are both missing the elements dorsal to the centrum, so the morphology of the centra is evident (fig. 12A). The centra are rectangular in dorsal view and slightly expanded transversely at both ends. The right lateral surface of the third caudal in CAGS 20-7-004 is exposed. Its centrum is slightly constricted midlength and is longer than those of the preceding two caudals. Visible at the anterior intervertebral articulation is a sharp beveling of the ventral margin to form chevron facets, as in *Velociraptor mongoliensis* (Norell and Makovicky, 1997) and *Deinonychus antirrhopus* (Ostrom, 1969). The prezygapophyses stretch slightly past the anterior surface of the centrum but do not display the extreme elongation seen in the distal caudals. The prezygapophyses are directed dorsally and taper distally. The transverse processes, in

lateral view, do not extend past the posterior margin of the centrum and appear more or less parallel to the dorsal surface of the centrum.

The transition from short anterior caudals to elongate posterior caudals begins at the sixth caudal in CAGS 20-8-001 (fig. 11). It is at this point also that the tail starts shifting its orientation in the slab, becoming visible laterally. The sixth caudal is the last to bear transverse processes and is intermediate in length between the elongate seventh caudal and short fifth caudal. The hyperelongate, rodlike extensions of the prezygapophyses and chevrons reach anteriorly as far as the third caudal, but elongation of both these elements begins around the sixth caudal; the orientation of the tail in the slab makes it difficult to tell where vertebral elongation starts. That the sixth caudal is the first to bear elongate prezygapophyses is corroborated by CAGS 20-7-004; in this specimen, the first chevron is situated between caudals 5 and 6, which suggests that caudal 6 is the first to have elongate prezygapophyses (fig. 12B). Thus, roughly three-quarters of the tail has elongated prezygapophyses, which is also true of *Deinonychus antirrhopus* (Ostrom, 1969), in which elongation begins at caudal 10. The *Deinonychus antirrhopus* tail has 36–40 vertebrae.

In both specimens, the distal caudals are preserved in lateral view, with thick bundles

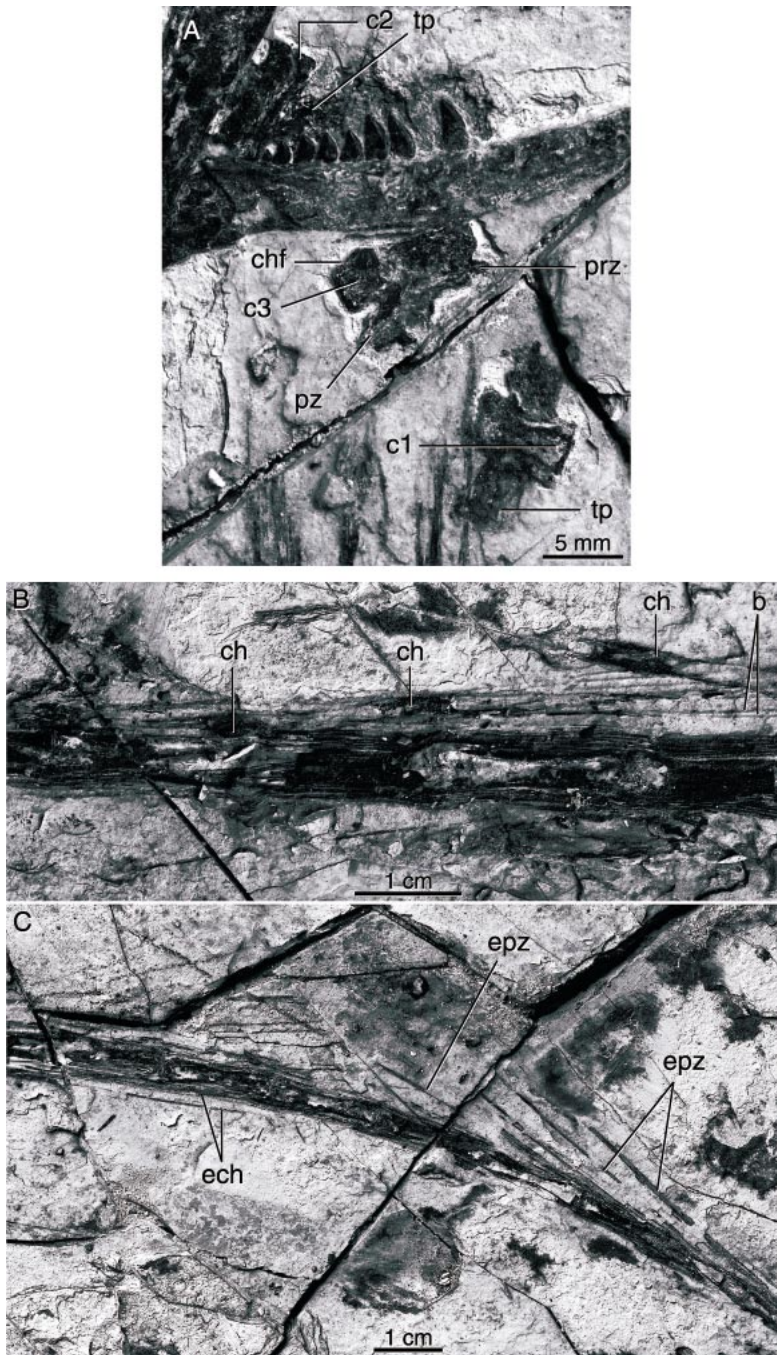


Fig. 12. Details of the tail of CAGS 20-7-004. (A) Anterior caudal vertebrae in various orientations. (B) Middle caudals in lateral view and isolated mid-caudal chevrons of CAGS 20-7-004 in dorsal view. (C) Bent distal portion of tail, showing snapped and disturbed caudal rods.

of caudal rods hiding the prezygapophyseal bases from view and the chevrons visible only as thickened wedges among the ventral set of rods (fig. 12B, C). In CAGS 20-7-004, two isolated mid-tail chevrons are exposed in dorsal view (fig. 12C). The main body of the chevron is roughly rectangular in this view and dorsally convex. Unlike the chevrons in *Deinonychus antirrhopus* (Ostrom, 1969), these have paired, extremely elongate posterior extensions in addition to their anterior extensions. The posterior extensions are shorter than the anterior ones and do not appear to bifurcate, but are at least three times the length of the body of the chevron. The posterior caudals are very long and have a smooth ridge along the midline of their lateral surfaces. The longest caudal is the sixth in CAGS 20-7-004 and the ninth in CAGS 20-8-001, fairly close to the proximal end of the tail. In both specimens, centrum length gradually decreases distally from the longest caudal.

The tail of *Microraptor* appears not to have the flexibility displayed by the tail in a specimen of *Velociraptor mongoliensis* (IGM 100/986), which is preserved in an S-shaped curve (Norell and Makovicky, 1999). The part of the tail wrapped by the caudal rods is completely stiff and straight in both the holotype (Xu et al., 2000) and CAGS 20-8-004. In CAGS 20-7-004, the distal end of the tail is bent laterally, but the caudal rods in this area do not follow the curvature of the tail as they do in IGM 100/986 (Norell and Makovicky, 1999). The caudal extensions have snapped and sprung apart at the apex of the bend, and they protrude stiffly from the vertebrae to which they are anchored (fig. 12D). The increased stiffening effect of the caudal rods would be expected to be greater at the smaller body size/mass of *Microraptor* than at the larger body size/mass of *Velociraptor*. The mechanical strength of the bone in the caudal rods would remain essentially the same per cross-sectional area at all sizes, but due to allometry, the relative force exerted on the caudal vertebrae would decrease as vertebral mass increased, since mass scales with volume, not area. Thus, at the larger body size of *Velociraptor*, the caudal rods would generate less tension on the tail vertebrae, allowing for more flexibility in the tail.

## RIBS

Dorsal and gastral ribs are splayed around the articulated dorsal vertebrae of CAGS 20-8-001 (fig. 13). The heads of the dorsal ribs are buried under the vertebrae, so the exact nature of the rib facets is unknown in this specimen. The expanded proximal portion of each rib is grooved longitudinally, and the proximal end of each rib tapers to a sub-millimeter width. The longest ribs are associated with the fifth through seventh dorsals; the ribs decrease in length as expected posteriorly along the series. Uncinate processes are preserved in their original positions among the ribs (fig. 14A, B). Xu et al. (2000) were not definitively sure that uncinates were present in the holotype. The uncinata processes have fan-shaped proximal ends and distally tapering shafts. They span three ribs each at an angle of approximately  $55^\circ$  and are not fused to the ribs to which they articulate. In life, the tapered ends of the uncinata processes would have pointed posterodorsally towards the spinal column. The visible gastralia appear to be single elements and are presumably the lateral gastral segments. These gastral segments are fairly long, about equal in length to the posterior dorsal ribs and longer than the sternal ribs.

CAGS 20-7-004 provides more information about the morphology of the ribs. A cervical rib, which touches the right side of the last cervical vertebra but is not in its correct articulated position, is typical of many coelurosaurian taxa (Makovicky, 1997). It is double-headed and broadly triangular proximally, with a blade that is shorter than the centrum of its associated vertebra (fig. 15A). An associated rib of the second dorsal has a very elongate capitular process and short tubercular process (fig. 15B). The rib shaft is short, as expected for a pectoral rib. The associated ribs of dorsals 4 through 7 are located nearby, and while they are not articulated with the vertebrae, they do appear to retain their original spacing and relative positions. These ribs have the longer shaft length and shorter capitular processes expected of mid-thoracic ribs (fig. 15C). Two uncinata processes identical in morphology to those in CAGS 20-8-001 are articulated with these ribs (fig. 14C). They also span

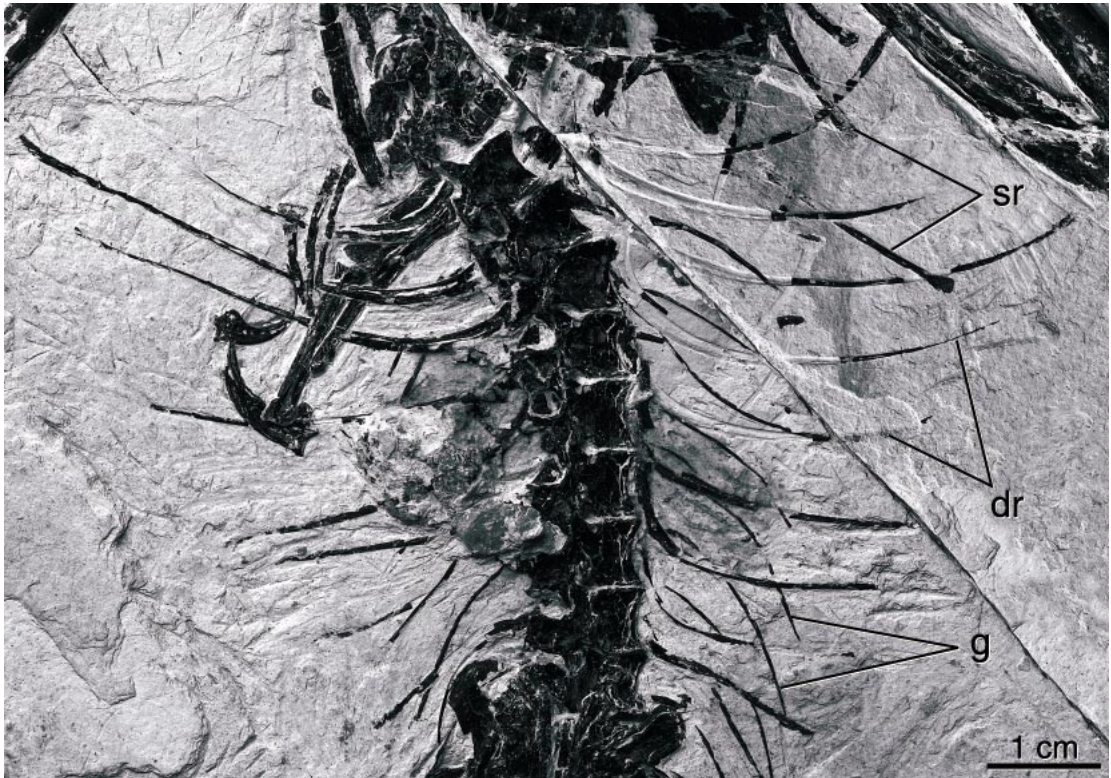


Fig. 13. Trunk of CAGS 20-8-001.

three ribs each but are angled at about  $70^\circ$  relative to the ribs, broader than the  $55^\circ$  angle seen in CAGS 20-8-001.

Uncinate processes have so far been definitively reported in only two other dromaeosaurids: *Velociraptor mongoliensis* (Paul, 1988; Norell and Makovicky, 1999) and NGMC 91, a recently described indeterminate dromaeosaurid that is very similar to *Sinornithosaurus* (Ji et al., 2001). The processes are most obviously preserved in the “Fighting Dinosaurs” specimen of *Velociraptor* (Kielan-Jaworowska and Barsbold, 1972; Unwin et al., 1995). In this specimen, the uncinate processes are much longer than those in *Microraptor*, spanning four ribs each at an angle similar to that observed in CAGS 20-8-001.

#### PECTORAL GIRDLE

The beautifully preserved pectoral girdle of CAGS 20-8-001 provides most of the information about this region (figs. 16, 17).

Both scapulocoracoids are preserved in oblique dorsomedial view (fig. 16). The L-shaped scapulocoracoid is similar in morphology to that of basal avialans *Archaeopteryx* (Wellnhofer, 1992, 1993) and *Confuciusornis sanctus* (Chiappe et al., 1999) and to that of *Sinornithosaurus milleni* (Xu et al., 1999). The scapular blade is long and strap-like but shorter than the humerus. The acromion is prominent but not laterally everted to a great extent. There is a deep fossa ventral to the acromion on the medial face of the scapula. Just anterior to the acromion, the coracoid is strongly inflected medially, giving the scapulocoracoid its distinctive “L” shape. The angle between the scapula and the coracoid in the dorsal plane is approximately  $105^\circ$ . The angle between the scapula and the coracoid in the dorsal plane is not reported for the three taxa listed above. However, the angle between the scapula and coracoid in the dorsal plane can be estimated for *Confuciusornis* from Chiappe et al. (1999: fig.

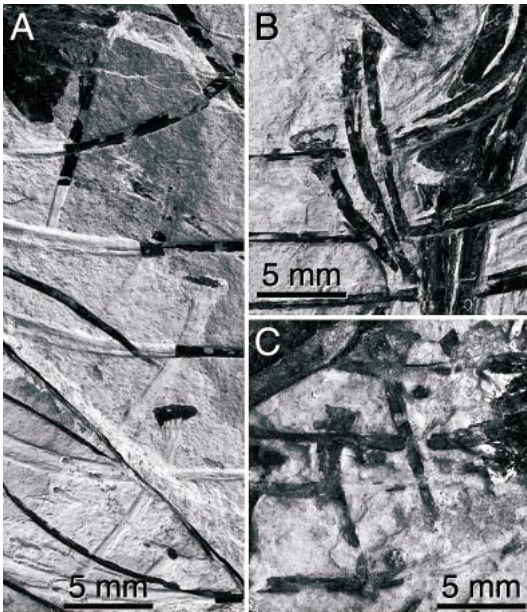


Fig. 14. Detail of uncinuate processes. Processes from the (A) right and (B) left sides of the rib cage of CAGS 20-8-001. (C) Processes from the left side of the rib cage of CAGS 20-7-004.

27) to be about  $95^\circ$ , similar to that of CAGS 20-8-001. The coracoid is completely fused to the scapula. Morphological details and ventral extent of the coracoids are hidden by matrix. Although neither coracoid is still articulated with the sternum, the medial inflec-

tion of the coracoid and the manner in which the left coracoid remains in contact with the sternum suggests the coracoid articulated to the anterior surface of the sternum (fig. 17A), as in *Velociraptor mongoliensis* (Norell and Makovicky, 1997).

Both sternal plates are preserved in CAGS 20-8-001 and are separate and unfused at their midline contact (fig. 17A). The sternum is shield-shaped, tapering posterior to the costal margin. Three widely spaced rib facets are clearly visible on the anterolateral edge of the right sternal plate (fig. 17B). These facets correspond to the three sternal ribs in close association with the plate, only one of which is actually articulated to the plate. At least one other facet is probably present on the plate: a fourth sternal rib, differentiable from the gastralia and thoracic ribs by its expanded, spoon-shaped distal end, lies just caudal to the posterior margin of the right sternal plate. Posterior to the costal margin, the sternum bears a short, laterally extending xiphoid process that is squared off at its distal end (fig. 17B). A similar process is present in *Confuciusornis* (Chiappe et al., 1999), *Velociraptor* (Norell and Makovicky, 1997, 1999), and oviraptorids (Clark et al., 1999).

The furcula of CAGS 20-8-001 is boomerang-shaped, with no trace of a hypocleidium at its apex (fig. 19A). The angle between the two rami of the furcula is  $91^\circ$ . The two arms

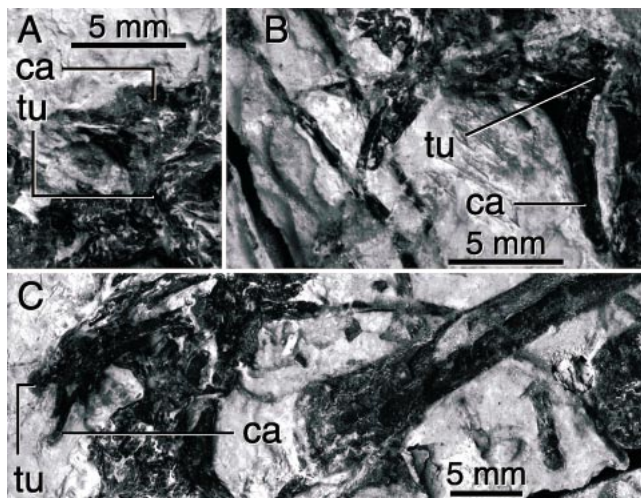


Fig. 15. Ribs of CAGS 20-7-004. (A) Cervical rib. (B) Pectoral rib. (C) Thoracic ribs.

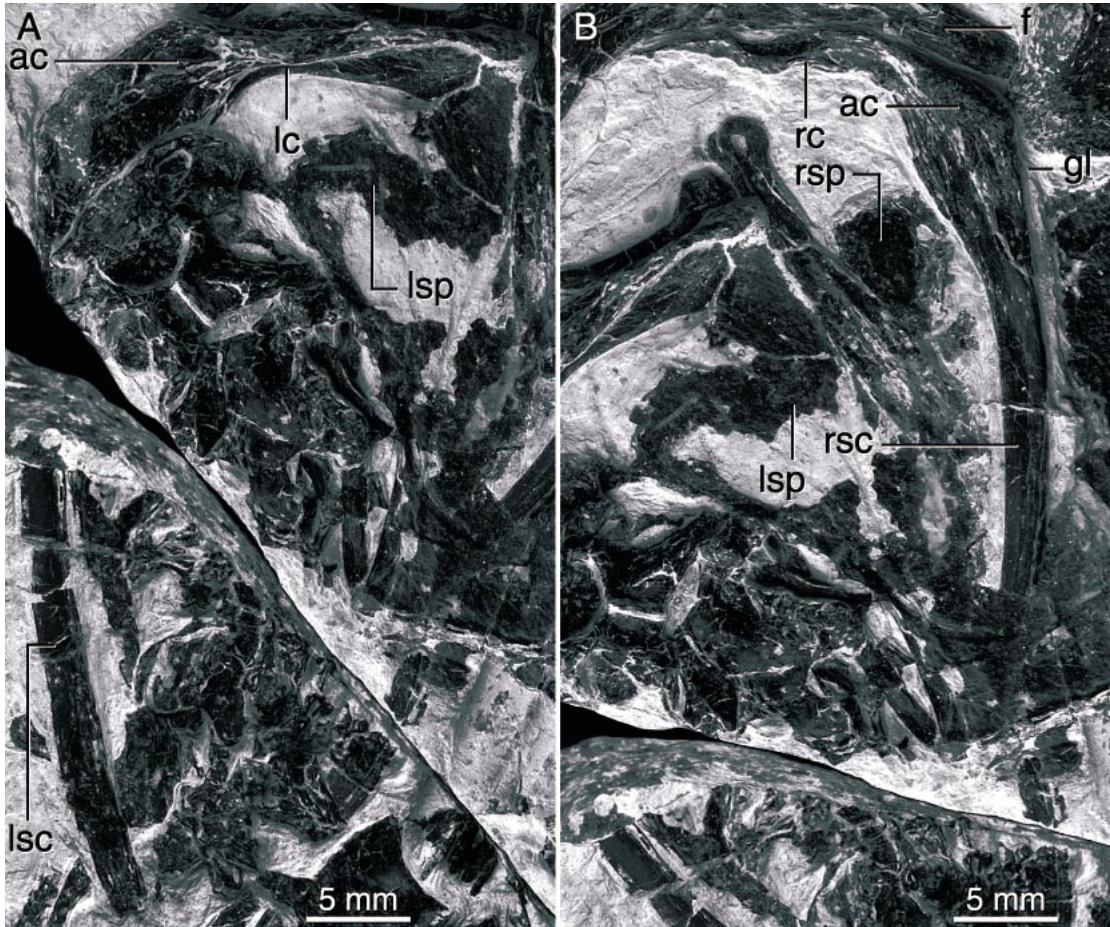


Fig. 16. Left (A) and right (B) scapulocoracoids of CAGS 20-8-001 in oblique dorsomedial view.

of the furcula broaden as they approach the point of fusion. The furcula is flattened dorsoventrally, although this may be influenced by preservation.

Poorly preserved fragments of an ossified sternum are present in CAGS 20-7-004, with sternal ribs associated with the right sternal plate (fig. 18). The sternum is widest at its anterior margin and tapers posteriorly. There appear to be four sternal ribs, which confirms the number identified in CAGS 20-8-001. The first sternal rib is articulated with the sternal plate at its anterolateral corner. Three other sternal ribs are in close association with the plate. The four small, triangular rib attachment facets present on the lateral margin of the sternum match the number of sternal ribs. Immediately posterior to the costal mar-

gin, the sternum is laterally expanded, but the sternal plate soon tapers again. The lateral expansion caudal to the rib attachment facets is probably the lateral xiphoid process seen in CAGS 20-8-001.

The sharply bent furcula of CAGS 20-7-004 lacks the gently curved “boomerang” appearance of the furcula of CAGS 20-8-001 (fig. 19B). The interclavicular angle of the furcula is  $82^\circ$ , compared to  $91^\circ$  for CAGS 20-8-001, but otherwise the morphology of the furcula is identical to that of CAGS 20-8-001. Makovicky and Currie (1998) reported a  $12^\circ$  difference in interclavicular angle between two different specimens of *Gorgosaurus libratus*, so the difference in interclavicular angles seen in the two *Microraptor* specimens may be normal intraspecific variation.



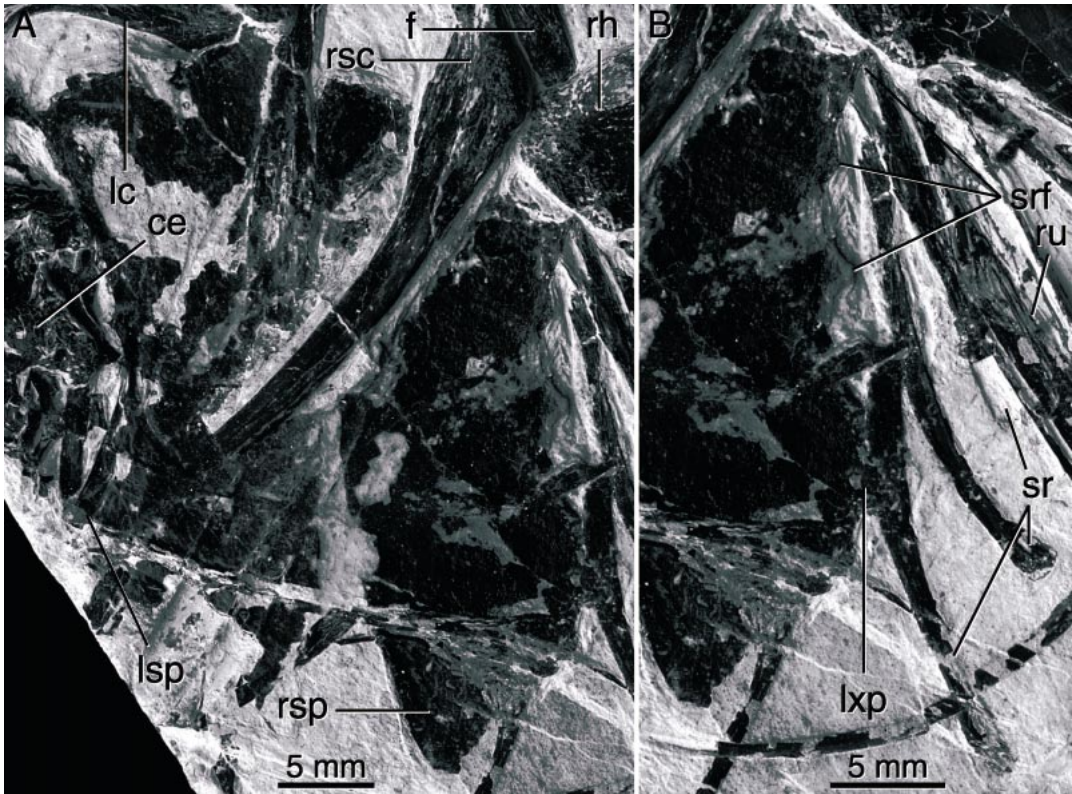


Fig. 17. Sternum of CAGS 20-8-001. (A) Left and right sternal plates. (B) Detail of lateral margin of right sternal plate.

There is no hypocleidium present at the apex of the furcula, and the two arms of the furcula broaden as they approach the apex. The right ramus articulates with a very poorly preserved fragment of the shoulder girdle. The large knob of bone above the proximal end of the right ramus may be the acromion. Two long, isolated flat bones near the top of the slab may be the two scapular blades of CAGS 20-7-004.

#### FORELIMB

The right humerus of CAGS 20-8-001 is complete and preserved in lateral view with the right radius and ulna folded beneath it (fig. 20). The distal end of the left humerus is preserved in lateral view in articulation with the left radius and ulna. The humerus of the specimen is long, and the shaft is only slightly thicker than that of the ulna. The proximal end bears a prominent head and

well-developed internal tuberosity. The internal tuberosity is approximately half the length of the deltopectoral crest and has a rugose lateral margin. The deltopectoral crest is also large and well-developed, extending one-third the way down the humeral shaft. The deltopectoral crest is expanded laterally for most of its length, coming to a point a few millimeters from its distalmost extent, so that the proximal end of the humerus is quadrangular in shape. The external (radial) condyle of the humerus is large and separated from the internal (ulnar) condyle by a deep groove extending several millimeters up the lateral surface of the shaft. The ectepicondyle appears to be present as a separate, narrow ridge paralleling the large radial condyle, but this may be a preservational artifact due to crushing. A small, round ligament pit is present on the lateral surface of the external condyle the humerus. From the impression

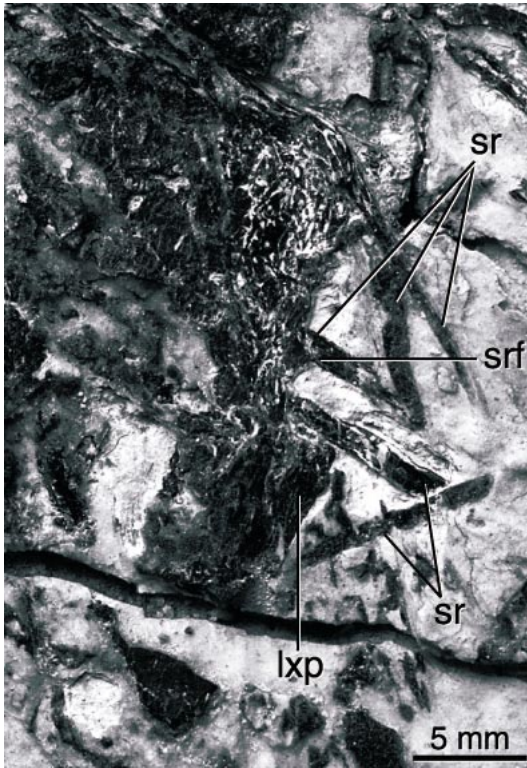


Fig. 18. Left sternal plate of CAGS 20-7-004.

that remains of the distal left humerus of CAGS 20-7-004, it appears that the distal condyles were well-rounded. The humerus of *Microraptor* is very similar in overall appearance to that of *Deinonychus* (Ostrom, 1969, figs. 55, 56).

The distal ends of the radius and ulna are not visible or present in either forelimb of

CAGS 20-8-001. Both radii and ulnae are preserved in lateral view. The radius and ulna are subequal in length to each other and to the humerus (fig. 20). The anteroposteriorly bowed ulnar shaft is approximately twice as thick as that of the radius, and it is expanded at its proximal end. In lateral view, the proximal surface of the ulna is sharply angled, slanting from the tip of the olecranon process towards the radius (figs. 20, 21). The olecranon is large and appears to fit into the groove between the radial and ulnar condyles of the humerus. The anterolateral part of the proximal articular surface, which contacts the radius, is laterally everted. In proximal view, the articular surface of the ulna is probably subtriangular, as in *Velociraptor mongoliensis* (Norell and Makovicky, 1999) and *Deinonychus antirrhopus* (Ostrom, 1969). The distal end of the right ulna of CAGS 20-7-004, which is missing its proximal end, is preserved, but the morphology is unremarkable. The distal articulation of the ulna is convex.

In CAGS 20-8-001, the articular ends of both radii are lost or buried under other elements (figs. 20, 21). Only the left radius is preserved in CAGS 20-7-004, and it has been split through the bone, so surface details are not visible. All that can be said about the radii is that they are expanded proximally.

Elements of the manus are scattered around the trunk of CAGS 20-8-001; many elements are missing and identification of individual phalanges and metacarpals is difficult due to their disarticulated state. Two

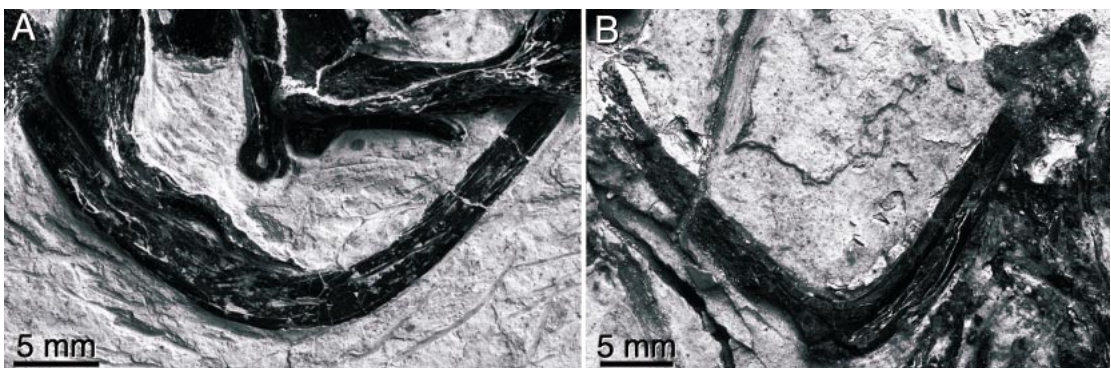


Fig. 19. Furculae of (A) CAGS 20-8-001 and (B) CAGS 20-7-004.

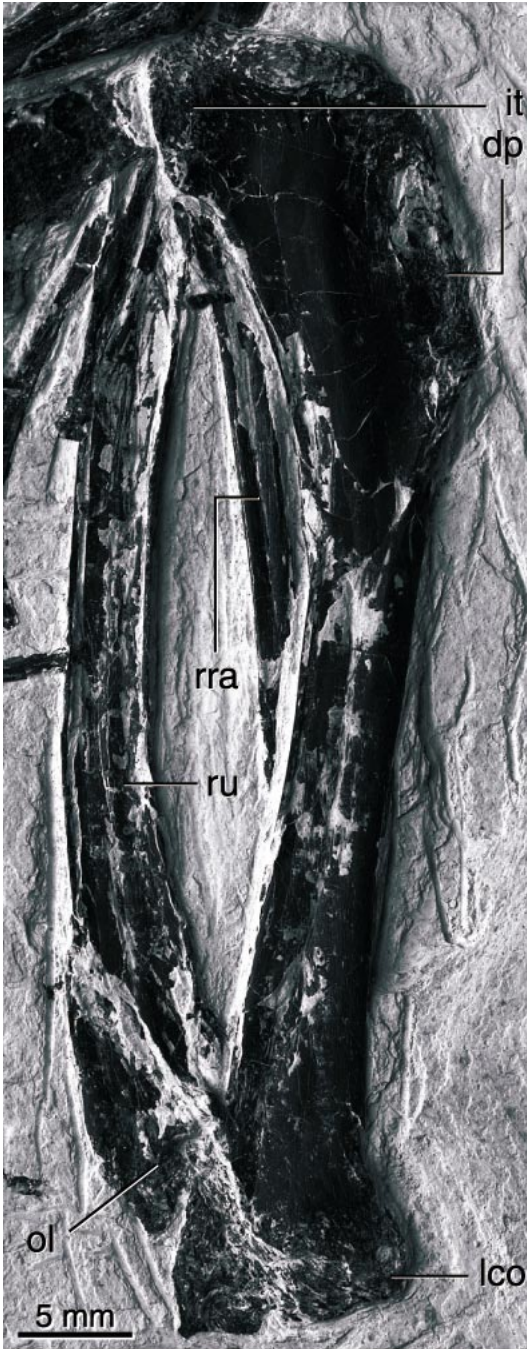


Fig. 20. Right humerus, radius, and ulna of CAGS 20-8-001 in lateral view.

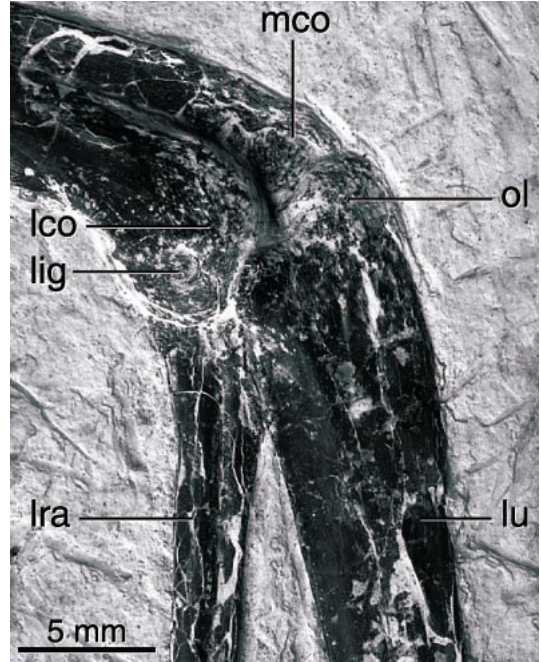


Fig. 21. Proximal portions of right radius and ulna of CAGS 20-8-001 in lateral view.

manual unguals, those of the first and probably second digits, are preserved along with their claw sheaths (fig. 22). The claw sheaths are extremely long and recurved; the sheath of the digit II unguis increases the length of the claw by almost 100%. The bony unguis of digit I is enormous, almost twice as long as that of digit II. Both unguis are strongly recurved, even without the claw sheaths, and have very large flexor tubercles.

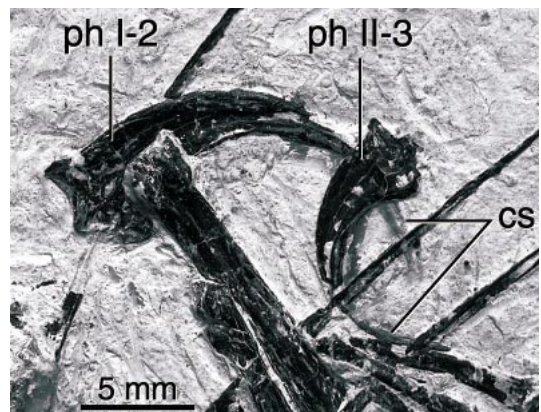


Fig. 22. Manual unguis of CAGS 20-8-001.

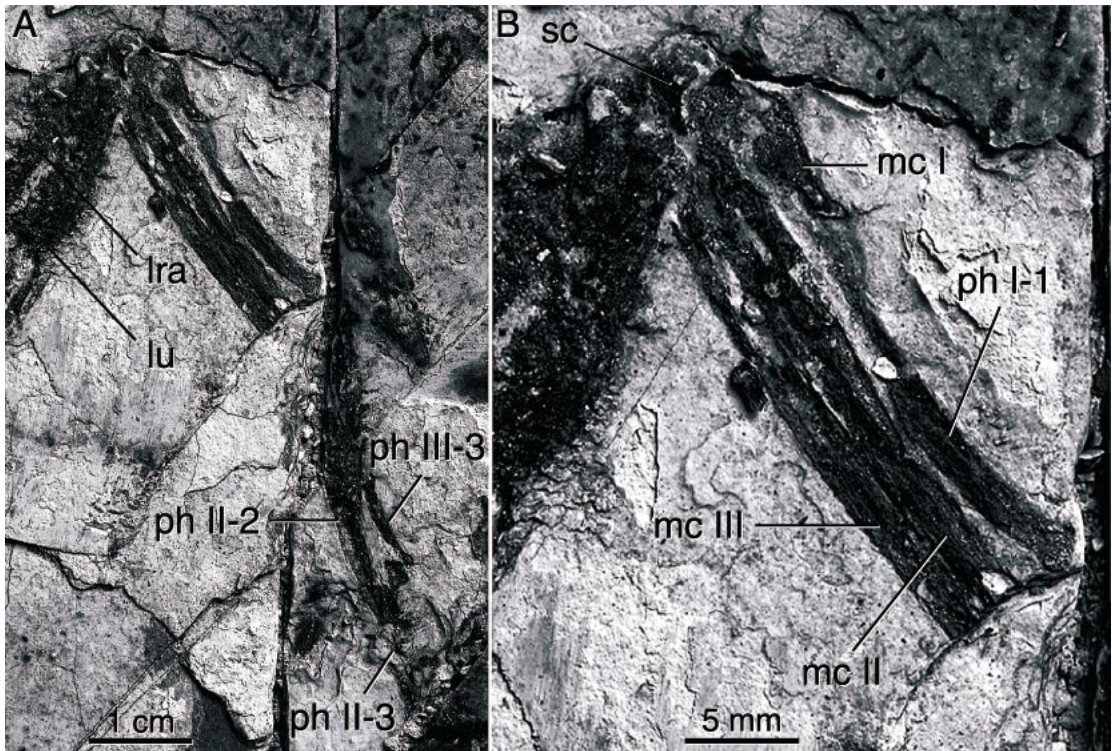


Fig. 23. Articulated left manus of CAGS 20-7-004. (A) View of metacarpals and phalanges. (B) Detail of wrist and metacarpals.

Only the left hand is articulated in CAGS 20-7-004, but preservation of both hands is poor (fig. 23). One carpal can be clearly seen in the wrist of the left hand, and it appears to be the semilunate carpal. The carpal is crescent-shaped, and it caps all of metacarpal I and part of metacarpal II. An isolated carpal in the region of the right hand is probably the right semilunate carpal. It is grooved proximally and is similar in morphology to the semilunate carpal of *Deinonychus antirrhopus* (Ostrom, 1969) and *Archaeopteryx lithographica* (Wellnhofer, 1974). It is impossible to tell whether the thickened region at the proximal end of metacarpal I is another carpal or simply the expanded proximal end of the metacarpal. Metacarpal I is expanded proximally and is only slightly stouter than the other two metacarpals. The first metacarpal is very short, as in other theropods, only about a third of the length of the long and slender metacarpal II. The distal ends of

metacarpals II and II are missing, but they are probably subequal in length.

*Microaptor* probably has a phalangeal formula of 2-3-4 as in most other theropods. The ungual of digit II is preserved in both hands of CAGS 20-7-004; all of the other manual unguals are missing. Phalanx I-1 is very long; it extends almost as far as the distal articulations of metacarpals II and III. It is subequal in thickness to metacarpals II and III. Digit II is the longest in the hand; the two phalanges are robust and elongated, with the penultimate phalanx slightly longer than phalanx II-1. The digit II unguals have large flexor tubercles and are strongly recurved. The separations between the phalanges of the third digit are difficult to see, but it appears as if the first phalanx is the longest and the second the shortest. The third phalanx of digit III is very slender, at midshaft only about half as thick as the preceding phalanx. Phalanx III-3 tapers distally from the wider prox-

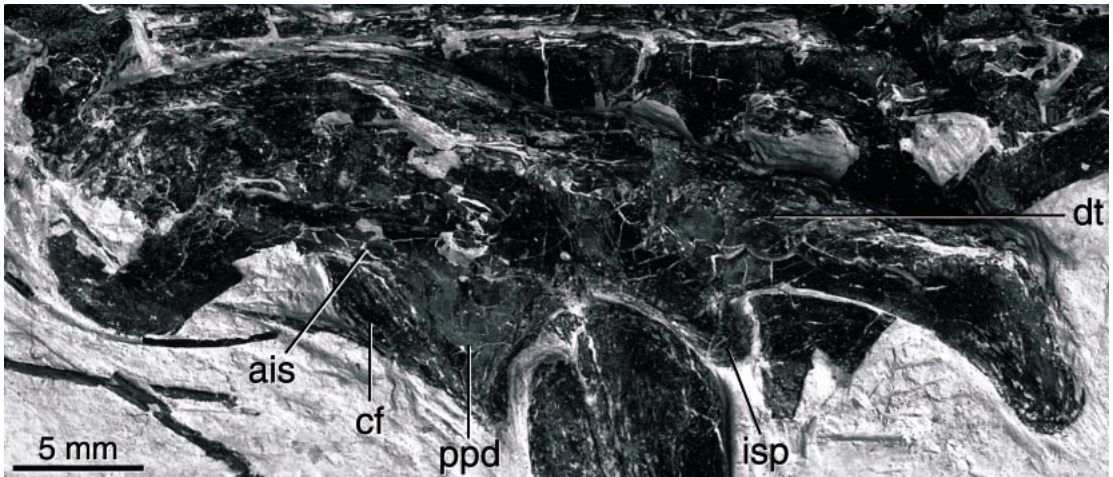


Fig. 24. Left ilium of CAGS 20-8-001 in lateral view.

imal articulation, which receives the equally wide distal trochlea of phalanx III-2.

#### PELVIC GIRDLE

In the holotype of *Microraptor*, only the ventral surface of the posterior iliac blades can be observed. In CAGS 20-8-001, both ilia are compressed so that their lateral surfaces are exposed dorsally (figs. 9, 24). The ilium is low and slender. The ilium is dolichoiliac, with the preacetabular process slightly longer than the postacetabular process. The anterior of the preacetabular process is gently rounded, with only a slight anteroventral hook, like the condition in *Velociraptor* (Norell and Makovicky, 1997, 1999). The antiliac shelf is reduced as in other dromaeosaurids, and no distinct cuppedic fossa is apparent. Instead, a slight lateral eversion of the ventral iliac margin that overhangs part of the pubic peduncle is present. The fossa beneath this lateral eversion is continuous with the large flat pubic peduncle (the preacetabular apron). The pubic peduncle is much larger than the ischiadic peduncle, approximately four times longer antero-posteriorly. The ventral margin of the pubic peduncle slopes posteroventrally. The dorsal rim of the acetabulum does not significantly overhang the head of the femur. The lateral surface of the ilium dorsal to the acetabulum is dorsoventrally concave. A vertical ridge dividing the anterior and posterior portions

of the ilium, as seen in some *Velociraptor* specimens (IGM 100-1982; see Norell and Makovicky, 1999) and many other theropods (Hutchinson, 2001), is not present.

In lateral view, the ischiadic peduncle is a weakly developed rounded protuberance with a small antitrochanter. The postacetabular wing of the ilium is dorsoventrally shorter than the preacetabular wing, which gives it a more slender appearance. The postacetabular process tapers posteriorly to a rounded point and hooks posteroventrally at its posterior end; its posterodorsal corner is sharply angled. The posteroventral tip of the postacetabular wing descends further ventrally than either peduncle. The lateral surface of the postacetabular process is concave. The preacetabular wings of the ilia are in contact with the neural spines of the first two sacrals, but this is probably due to the post-mortem dorsomedial shifting of the ilia. The postacetabular alae of the ilia diverge laterally, as in other dromaeosaurids (Norell and Makovicky, 1997).

The articulated pubes are preserved in posterior view and, unlike the holotype, CAGS 20-8-001 preserves the pubes' distal extremities (fig. 25). In areas of overlap, the pubes in CAGS 20-8-001 closely approximate conditions observed in IVPP V12330. The proximal articulation has a broad sub-rectangular dorsal surface that slants posteroventrally. The slanting surface would artic-

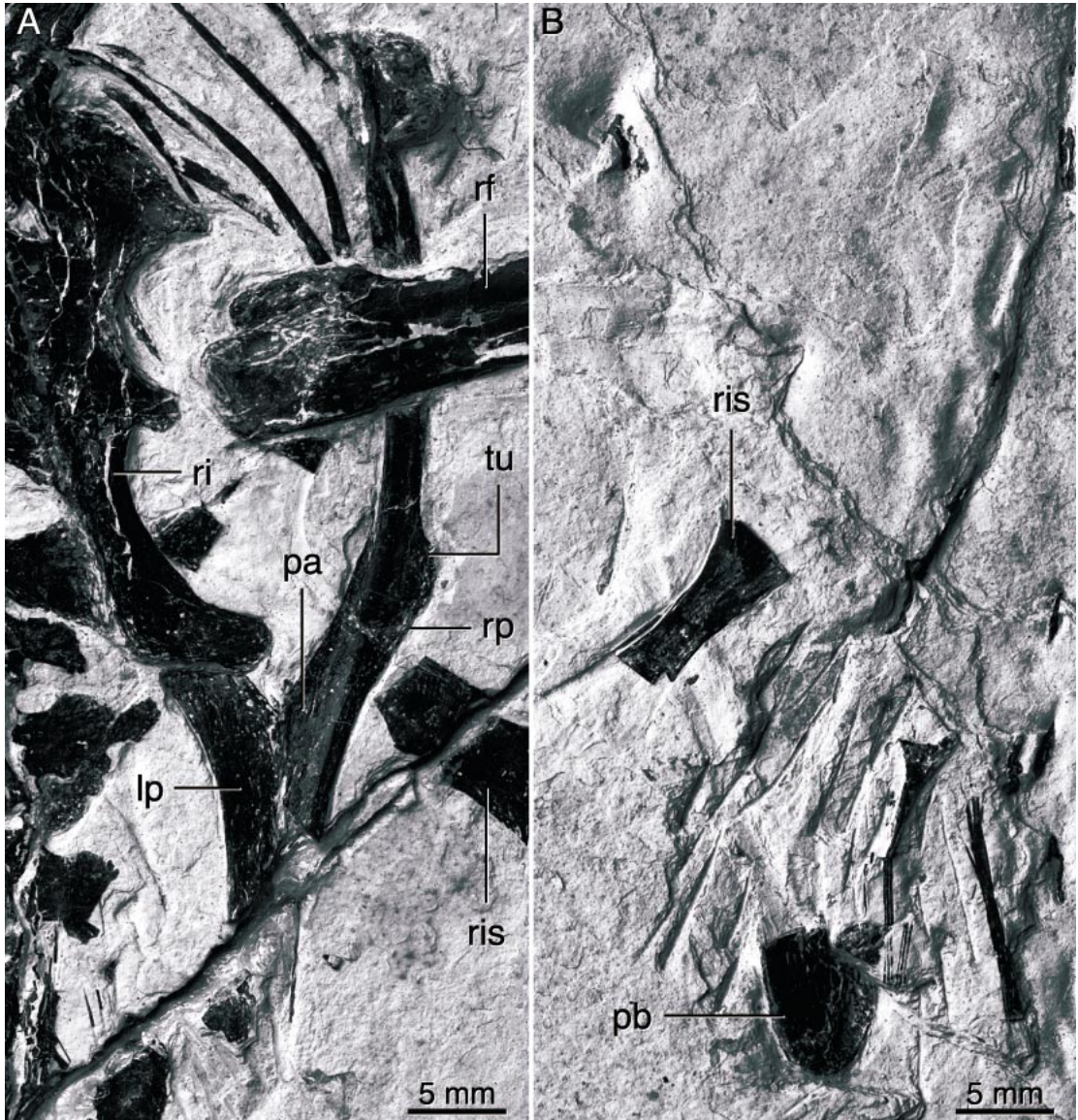


Fig. 25. Articulated pubes of CAGS 20-8-001. (A) Pubic elements preserved on the slab, posterior view. (B) Distal symphysis preserved on the counterslab, anterior view.

ulate well with the posteroventrally sloping pubic peduncle on the ilium to project the pubes distally to form the opisthpubic condition typical of dromaeosaurids. The pubic shaft is anteroposteriorly flattened. A wide pubic canal, typical of advanced maniraptorans (Norell and Makovicky, 1997), is present. Halfway down the length of the shaft, the medial edge begins to thin and extend

medially, joining the opposing pubis to form the pubic apron. Just proximal to the pubic apron the lateral edge of the shaft also expands into a small tubercle like that in *Sinornithosaurus* (Xu et al., 1999). Each half of the apron curves posteriorly at its proximal end, so that at the midline the halves meet at a posteriorly directed contact, as in *Velociraptor* (Norell and Makovicky, 1997)

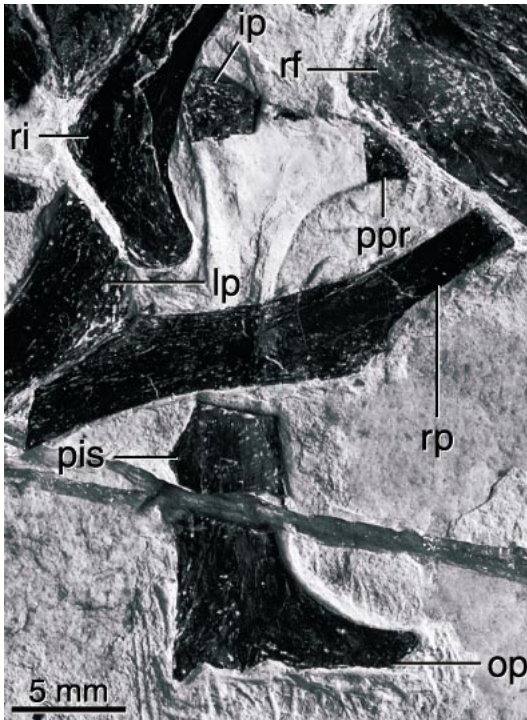


Fig. 26. Right ischium of CAGS 20-8-001 in lateral view.

and *Unenlagia* (Novas and Puerta, 1997). The apron becomes flatter distally and ends in a flattened symphysis that is crushed so that the right lateral surface is exposed. On the counterslab, a small pubic boot with no anterior expansion is observed (fig. 25B).

Both ischia are preserved, the right in lateral view and the left in medial view, although much of the left ischium is obscured by overlying elements (fig. 26). They are identical to the ischia of the holotype. The ischia are short, approximately half the length of the pubes, as in the type specimen and other dromaeosaurs. Like in *Archaeopteryx* and most other maniraptorans, the ischia were apparently distally unfused. The proximal end of the ischium is expanded anteroposteriorly. The pubic process is substantially longer than the iliac process, but since the iliac process does not extend significantly from the ischiadic shaft, the proximal end of the ischium is more L- than T-shaped in lateral view. The iliac and pubic processes are separated by a short concave area that is the

ischadic contribution to the acetabulum. As in the holotype, *Sinornithosaurus* (Xu et al., 1999), *Archaeopteryx* (Wellnhofer, 1974), *Rahonavis* (Forster et al., 1998), *Unenlagia* (Novas and Puerta, 1997), and *Sinovenator* (Xu et al., 2002), a small triangular posterior process is present on the posterior edge of the ischium, the apex of which is located approximately two-thirds down the shaft. A large obturator process is confluent with the distal margin of the ischium, causing the distal end to be L-shaped in lateral view as well. It is likely that the long obturator process contacts the pubis. The ischium is flat and platelike, and the shaft curves slightly anteriorly in lateral view.

The pelvis is badly crushed and poorly preserved in CAGS 20-7-004. As a result, it yields no morphological information. The ischia and pubes, though in slightly better condition, are incomplete and yield no additional information.

#### HINDLIMB

IVPP V12330 preserves only the fragmentary proximal ends of the right and left femora, which are exposed medially. In CAGS 20-8-001 the left femur is preserved in articulation with the pelvis in its entirety, while the right femur is preserved a few millimeters from the pelvis with its distalmost end missing. The proximal two-thirds of the left femur are located on one slab in lateral view, while the distal end is on another slab in medial view (fig. 27A, C).

The greater trochanter of the femur is broad and separated from the cylindrical lesser trochanter by a distinct groove, more like the condition in *Archaeopteryx* than that in *Velociraptor* (Norell and Makovicky, 1999). The dorsal margin of the lesser trochanter is approximately 2 mm below that of the greater trochanter. A small accessory crest is present at the base of the lesser trochanter, forming a sharp lateral corner at the base of the lesser trochanter, as noted in IVPP V12330 by Xu et al. (2000). The rugose posterolateral region of the femur just below the dorsal surface of the greater trochanter is probably the posterior trochanter. The lateral ridge (sensu Norell and Makovicky, 1999) is present as a large rugose bump

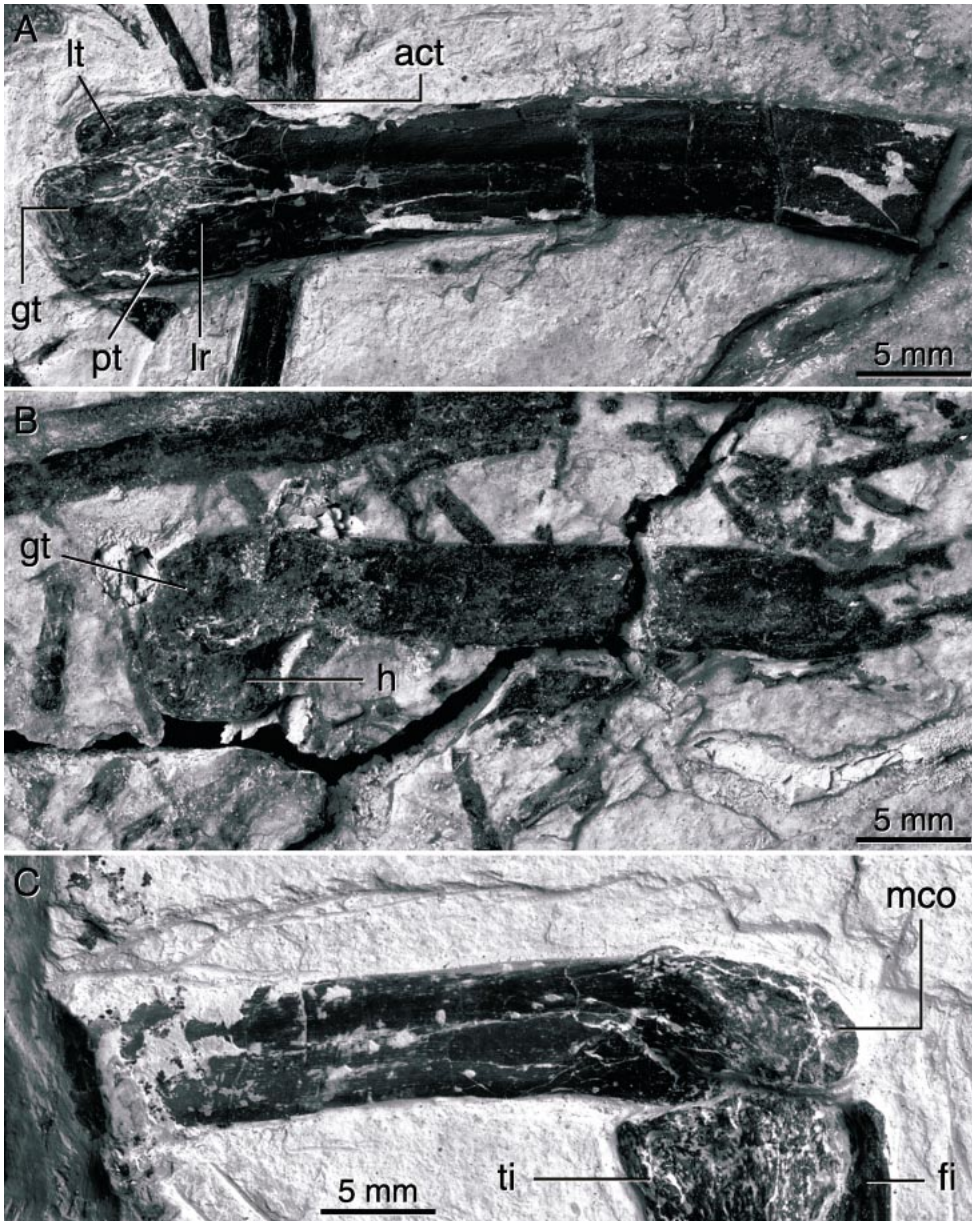


Fig. 27. Femur of *Microraptor*. (A) Proximal end of right femur of CAGS 20-8-001 in lateral view. (B) Proximal end of left femur of CAGS 20-7-004 in anterior view. (C) Distal end of left femur of CAGS 20-8-001 in medial view.

on the lateral surface of the femur a few millimeters below the apex of the greater trochanter. The lateral ridge does not lead into a longer ridge ventrally as in *Velociraptor* (Norell and Makovicky, 1999). Proximal to the lateral ridge, the entire lateral surface of

the femur, including that of the lesser trochanter, is concave and moderately rugose. A transverse rugose ridge separates this concave area from the smooth cortical bone of the rest of the shaft. The femoral shaft is anteroposteriorly bowed as in the holotype and



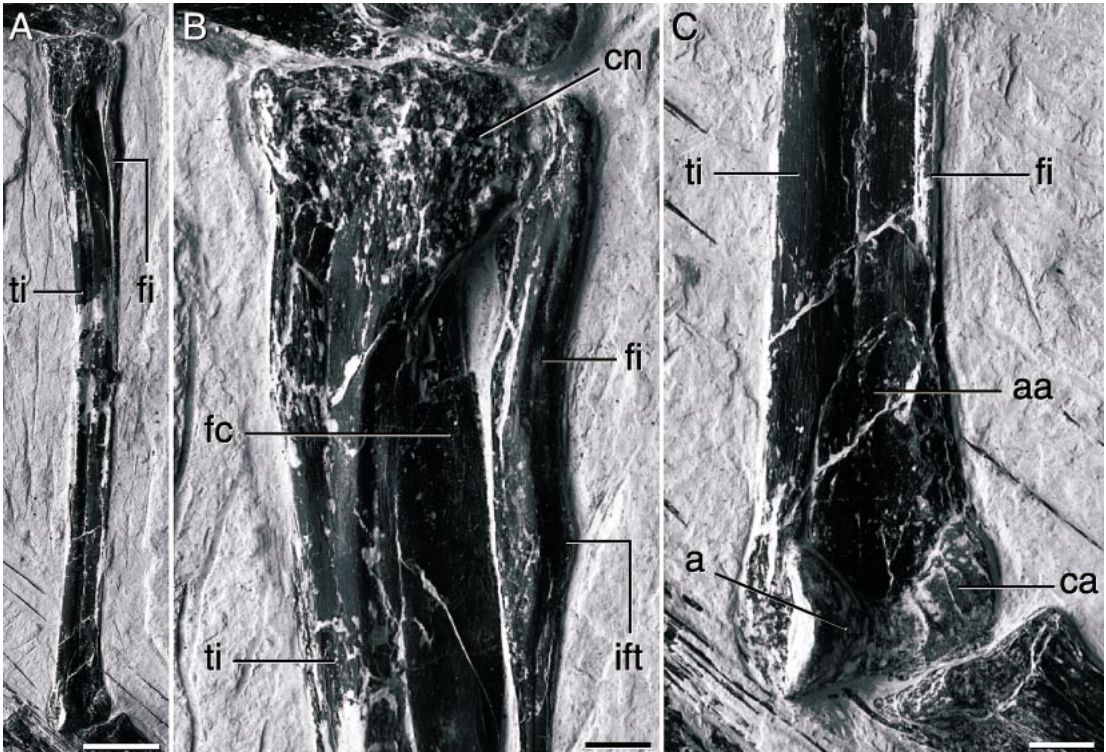


Fig. 28. Left tibiotarsus and fibula of CAGS 20-8-001. (A) Anterior view. Scale bar = 1 cm. (B) Detail of proximal tibia and fibula. Scale bar = 2 mm. (C) Detail of astragalus and calcaneum. Scale bar = 2 mm

most other maniraptorans. Only the medial condyle is visible in this specimen. It is not anteroposteriorly expanded to a great extent, so that in medial view it is oval in shape rather than round and does not extend posteriorly beyond the shaft.

The left femur of CAGS 20-7-004 is preserved within the slab with its anterior surface visible, while the right femur is twisted in the slab so that the posterior surface is visible proximally and the posteromedial surface is visible distally. The femur head has a distinct ventral lip and is continuous with the greater trochanter on the dorsal surface (fig. 27B). The medial condyle of the right femur is well rounded but does not protrude beyond the shaft posteriorly, like the medial condyle of CAGS 20-8-001. The medial condyle of the left femur is missing, but its impression remains, indicating that the lateral condyle was the larger of the two. Both condyles are

large and expanded beyond the lateral and medial margins of the femoral shaft.

The left tibiotarsus and fibula are excellently preserved in anterior view in CAGS 20-8-001 (fig. 28). The tibia is long and straight, approximately 128% longer than the femur, as noted by Xu et al. (2000) in the holotype. Proximally, the tibia is expanded (fig. 28B). The proximal tibia bears a well-developed single cnemial crest that has a pitted and rugose anterior surface. The cnemial crest extends a short distance onto the tibial shaft. The short, proximally placed fibular crest rises slightly from the tibial shaft.

The proximal fibula is concave medially, with no deep medial fossa (fig. 28B). The iliofibularis tubercle is prominent on the lateral surface of the fibula. The midpoint of the fibular crest of the tibia is level with the iliofibularis tubercle. The fibular shaft above and below the iliofibularis tubercle is medio-

laterally expanded so that it is the widest part of the fibula. Distal to the iliofibularis tubercle, the fibular shaft rapidly thins to a sub-millimeter-wide splint that is tightly appressed to the tibia. The distal end of the fibula contacts the calcaneum.

The astragalus is fused to the calcaneum, and both are fused to the tibia (fig. 28C). The ascending process of the astragalus is paper-thin and covers most of the anterior surface of the distal tibia. The ascending process tapers slightly at its proximal end, and its apex is positioned laterally on the anterior surface of the tibia, not centered. Laterally, the ascending process contacts the fibula. A faint line is present between the astragalus and the calcaneum, and may be the suture between these bones. Part of the distal extremity of the lateral condyle of the astragalus is covered by the metatarsals, but it appears the medial condyle is larger than the lateral one. The two well-developed condyles are separated by a shallow sulcus but are confluent with each other. A deep groove separates the condyles from the ascending process proximally, as in all coelurosaur.

The tibiotarsi and fibulae of CAGS 20-7-004 provide no additional information about these elements; the tibia of this specimen is 126% longer than the femur, comparable to the ratio of 128% seen in IVPP V12330 and CAGS 20-8-001.

The distal tarsals and proximal metatarsals are preserved only for the left foot of CAGS 20-8-001 (fig. 29A). The flat, platelike distal tarsals are fused to the metatarsals; only the medial tarsal is visible in this specimen. A faint suture can be seen between the medial distal tarsal and metatarsal II. Fusion to metatarsal II is strongest at the anterior margin, where there is no trace of the separation between the two elements. This is different from the condition in *Velociraptor*, in which the distal tarsals cap metatarsals III and IV, fail to reach the anterior margins of the metatarsals, and are most strongly fused to the posterolateral edges of metatarsals III and IV (Norell and Makovicky, 1999). The distal tarsal overhangs the posterior margin of metatarsal II by a substantial distance, as in *Velociraptor* (Norell and Makovicky, 1999). The proximal surface of the distal tarsal is more or less horizontal, but the distal surface

slopes posteroventrally so that the posterior margin of the tarsal is thicker than the anterior. The fourth metatarsal also appears to be fused to the distal tarsals.

In CAGS 20-8-001, the left pes is oriented in oblique posteromedial view in such a way that the proximal end of the third metatarsal is hidden between the second and fourth metatarsals (fig. 29A). Only the left pes is preserved in CAGS 20-7-004, as the slab ends abruptly at the distal end of the right tibiotarsus. Some crushing of the metatarsals is present, and there is a transverse break approximately one-third of the way down the metatarsus that cuts through all four of the visible metatarsals (fig. 29B). However, metatarsals II through V are visible in anterior view, which provides additional information about the metatarsus. The metatarsals are long and slender. The third metatarsal is the longest, the second the shortest, and the fourth is slightly shorter than the third. Metatarsal II is slender and laterally compressed, and metatarsal IV is the stoutest of the metatarsal elements, as in troodontids (Osmólska and Barsbold, 1990). The proximal end of metatarsal II is slightly expanded, with a small anterior lip. The distal articular surface of metatarsal II is ginglymoid. Xu et al. (2000) described the feet of IVPP V12330 as having a proximally compressed metatarsal III that contributes to the ankle joint, a “partially arctometatarsalian” condition similar to the one described for *Sinornithosaurus* (Xu et al., 1999). The arctometatarsalian nature of the pes cannot be verified by either specimen, as the proximal end of the metatarsal III is hidden in CAGS 20-8-001, and in CAGS 20-7-004 metatarsals III and IV are severely crushed. The distal articulation of the third metatarsal is ginglymoid, although not as obviously as that of metatarsal II. The fourth metatarsal has a posteriorly directed flange positioned at midshaft. The proximal end is expanded laterally. The distal articulation of metatarsal IV is overlapped by other elements in CAGS 20-8-001 and split along the center in CAGS 20-7-004, so its morphology cannot be determined. The fifth metatarsal is a long, thin splint that is in contact with the fourth metatarsal proximally for approximately one-third of its length. Distal to the area of contact with metatarsal IV,

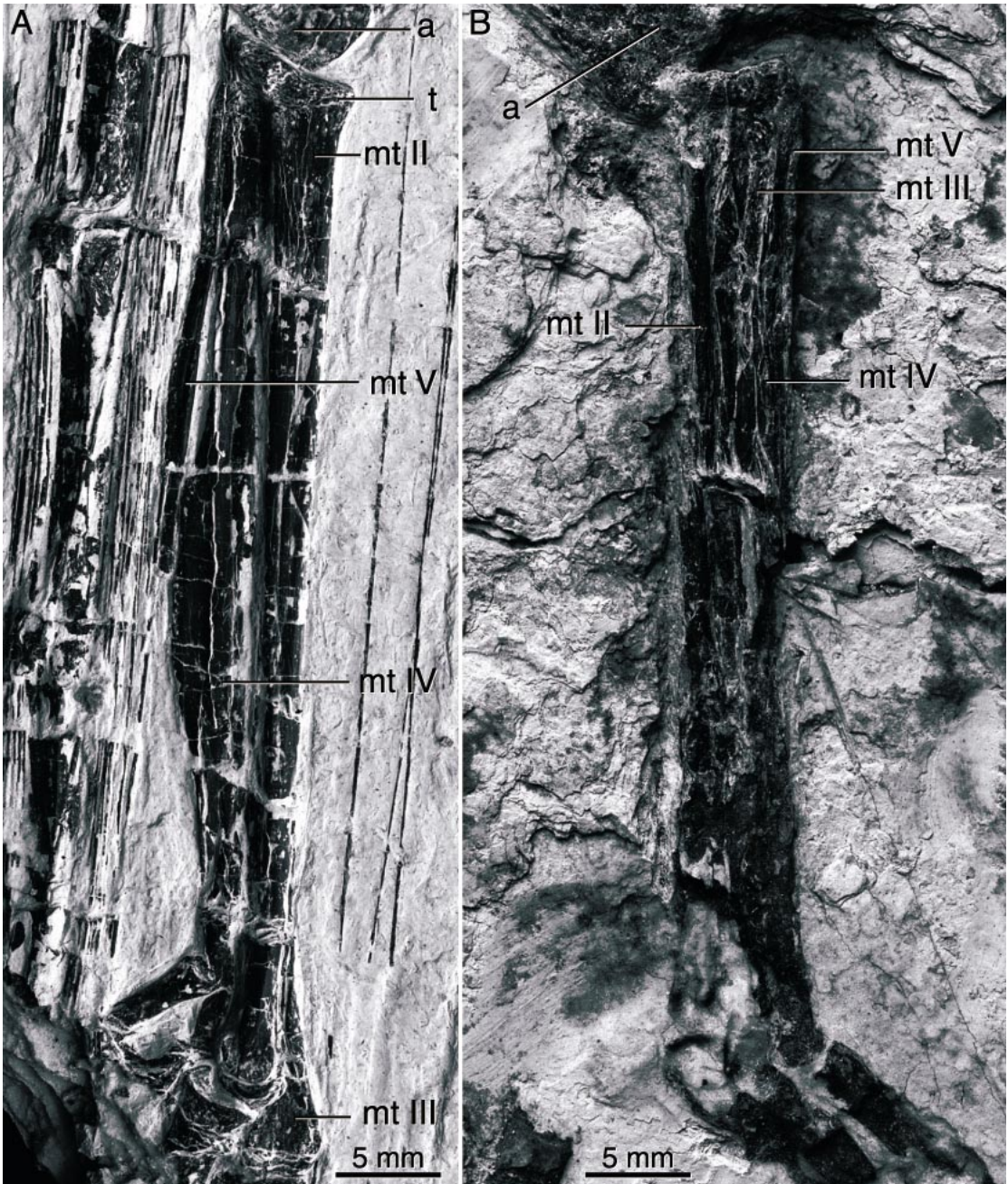


Fig. 29. Tarsals and metatarsals of *Microraptor*. (A) Left distal tarsals and metatarsals of CAGS 20-8-001 in oblique posteromedial view. (B) Left metatarsals of CAGS 20-7-004 in anterior view.

metatarsal V bows posteriorly, coming into contact again with metatarsal IV at its distal end. The shaft of metatarsal V is expanded at its bowed region. A slender metatarsal I is

positioned on the posterior surface of metatarsal I (fig. 30). Because the specimen is not preserved three-dimensionally, it is impossible to determine whether or not digit I is re-

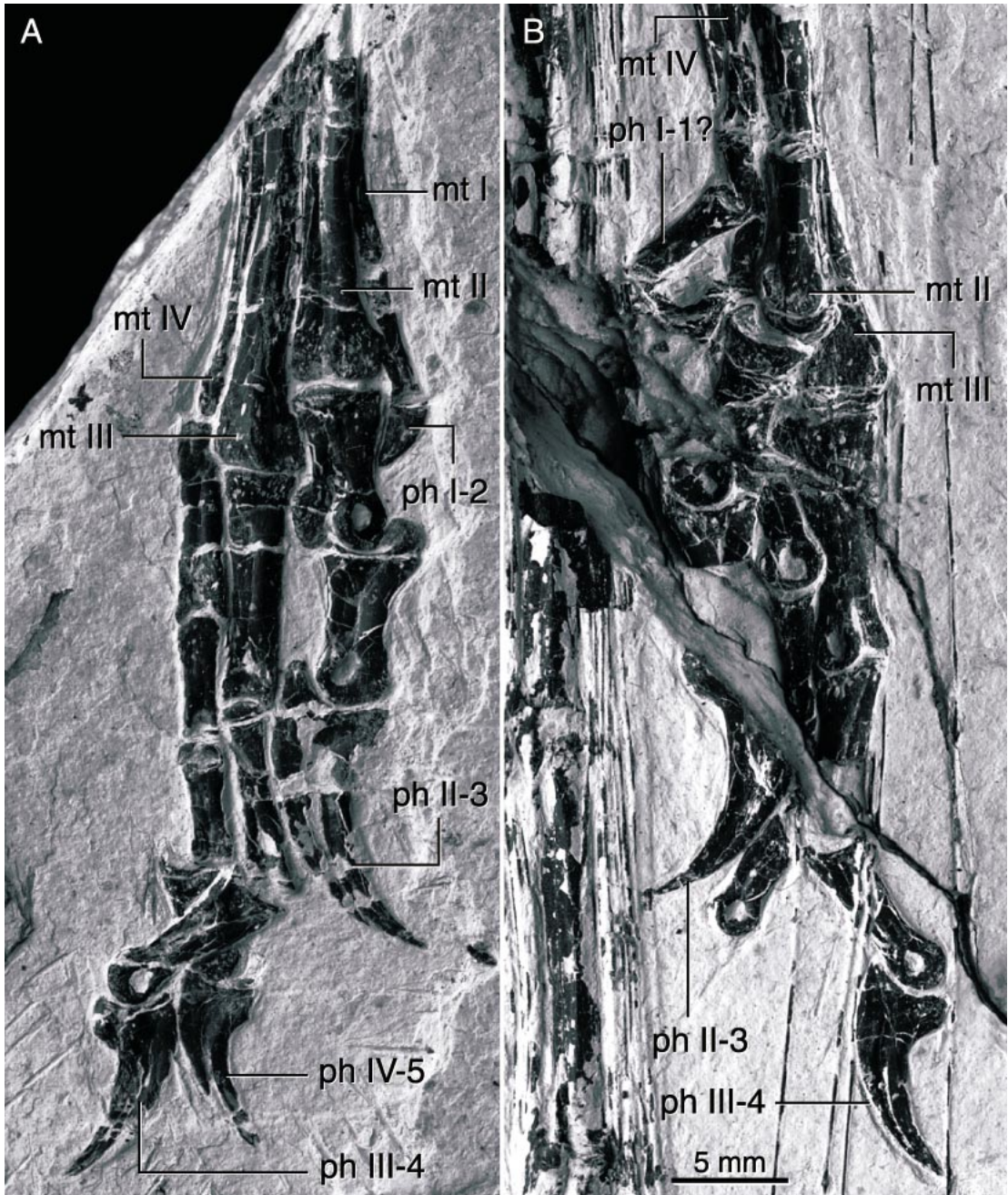


Fig. 30. Pedal phalanges of CAGS 20-8-001. (A) Right and (B) left feet in oblique posteromedial view.

versed due to compression of the specimen (Middleton, 1999). Metatarsal I is placed very close to the proximal end of metatarsal II, so that the distal tip of the ungual of digit

I reaches only to the midpoint of phalanx II-1. The proximal end of metatarsal I is hidden behind metatarsal II but appears to attenuate to a point, as in other dromaeosaurids.

All of the phalanges in the right foot in CAGS 20-8-001 are well preserved (fig. 30A). The first digit is short and slender, with an ungual that is far smaller than any of the other digits. The second digit displays all of the typical dromaeosaurid characters. Phalanx II-1 is very wide and robust in comparison to the phalanges in the other digits. Its distal articulation bears a well-developed ginglymus, with a very deep groove separating the two condyles. This groove extends onto the anterior surface of phalanx II-1. Phalanx II-2 has a prominent ventral heel at the base of its proximal articulation. The distal condyles are tall, and the ligament pit on the medial surface is placed dorsally. The ungual is characteristically hypertrophied and recurved strongly. A large flexor tubercle is positioned ventral to the deep articular facet. The third and fourth digits are similar in appearance: both are long and slender. Including the unguals, digits III and IV contain four and five phalanges, respectively. Phalanx III-1 is the longest phalanx in the pes, while phalanges III-2 and III-3 are subequal in length. The phalanges in digit IV decrease in length distally. The unguals of digits III and IV are identical in morphology, with ungual III-4 only slightly larger than IV-5. Unguals III-4 and IV-5 are similar in morphology to II-3, with large flexor tubercles and high degrees of curvature. The only difference is that their articular facets are not as deep as that of the second ungual. What can be observed on the fragmentary remains of the foot in CAGS 20-7-001 confirms the morphology seen in CAGS 20-8-004.

## DISCUSSION

### ANATOMICAL FEATURES

Xu et al. (2000) noted several avian affinities of *Microraptor* in their original description: waisted teeth with loss of serrations, a platelike ischium with a posterior process and distal obturator process, enlarged sacrals, and a reduced number of caudal vertebrae. The discovery of CAGS 20-7-004 and CAGS 20-8-001 allows us to add several more similarities to the list: a sharply bent scapulocoracoid, a laterally facing glenoid, a humerus longer than the scapula, a sternum that articulates with the coracoid anteriorly,

free uncinat processes, and a reduced antiliac shelf. The new specimens of *Microraptor* also confirm some of the troodontid affinities noted by Xu et al. (2000), such as waisted posterior teeth with serrations only on the posterior carinae, a robust fourth metatarsal, and a laterally compressed second metatarsal. *Microraptor* is especially similar in morphology to *Sinovenator* (Xu et al., 2002), the most basal known troodontid. Both animals have completely unserrated anterior maxillary and dentary teeth (Xu et al., 2000), teeth that are slightly inset medially, denticles of the same relative size, no pneumatic foramina on the dorsal centra, L-shaped scapulocoracoids with laterally facing glenoids, opisthopubic pelvis, ischia with distally positioned obturator and posterior processes, and partially arcotmetatarsalian feet. This study (see below) corroborates the finding of Xu et al. (2000) that *Microraptor* is the most basal dromaeosaurid known, so the large number of similarities between *Microraptor* and *Sinovenator* is not surprising. These two taxa, the basalmost of their respective clades, are probably very close to the basal deinonychosaur split and thus retain many primitive ancestral characters.

In comparison with other dromaeosaurids, the presacral vertebrae of *Microraptor* are very unusual. Carotid processes have not previously been found on other dromaeosaurid cervical vertebrae (Norell and Makovicky, in press), but they are clearly visible in CAGS 20-7-004. The elongated centra of the dorsals are more similar to those of *Archaeopteryx* and *Rahonavis* than to the blocky centra of other dromaeosaurids. The lack of pneumatic foramina in the dorsal vertebrae of *Microraptor* is also unusual for dromaeosaurids.

Most tetanuran theropods have pneumatic foramina on the centra of the axis, cervicals, and anteriormost dorsals; some tetanurans, including dromaeosaurids, have pneumatic openings on all presacral (postatlantal) vertebrae (Britt et al., 1998). The cervical vertebra preserved in CAGS 20-7-004 appears to be pneumatized, but the anterior dorsals of both specimens are not in the correct orientation to determine whether or not the anteriormost thoracic vertebrae are pneumatic as well. We can assume that *Microraptor* pos-

sesses only pneumatic cervicals and that the anterior thoracic vertebrae like the primitive tetanuran condition. The distribution of pneumatic trunk vertebrae in the basal Avialae-Deinonychosauria clade is complex. Other dromaeosaurids, such as *Velociraptor*, *Deinonychus*, *Saurornitholestes*, and *Unenlagia* (Norell and Makovicky, 1999), have large pneumatic foramina on all their dorsal centra. Like *Microraptor*, most troodontids, which are emerging in our recent phylogenetic analyses as sister taxa to Dromaeosauridae (this study; Xu et al., 2002), and *Archaeopteryx* (Britt et al., 1998) display the primitive tetanuran pattern of vertebral pneumaticity. However, *Confuciusornis* (Chiappe et al., 1999) and *Rahonavis* (Forster et al., 1998), both basal avialans, have pneumatic thoracic vertebrae. *Archaeopteryx*, *Microraptor*, and *Sinovenator*, which all lie close to the basal paravian divergence, may retain the apneumatic thoracic vertebrae of their common ancestor while later members of their respective clades evolved pneumatic dorsal centra.

The distribution of uncinete processes within the Theropoda has been indeterminate, because they are fragile elements that are often not preserved. As mentioned previously, within the Dromaeosauridae, uncinete processes have been definitively found in *Velociraptor mongoliensis* and NGMC 91. A ventral rib of *Deinonychus* (Ostrom, 1969: fig. 52A) was considered by Paul (1988) to be an uncinete process, but because this specimen is no longer articulated, this reinterpretation is uncertain. The only other non-avian theropod group in which uncinete processes have been found is Oviraptoridae. Uncinete processes are present in multiple specimens of at least two species: *Citipati osmolskae* (IGM 100/979, Clark et al., 1999; and IGM 100/1004, personal obs.) and *Khaan mckennai* (IGM 100/1127 and IGM 100/1002, Clark et al., 2001). The basal avialan *Confuciusornis* also has free uncinete processes like those seen in non-avian theropods (Chiappe et al., 1999). However, uncinetes are unknown in *Archaeopteryx*.

The increasing number of non-avian theropod and *Confuciusornis* specimens found with uncinete processes support Chiappe et al.'s (1999) hypothesis that the absence of

uncinete processes in other basal avialans is due to preservational factors or ontogenetic development and that ossification of these processes is primitive for Avialae, perhaps even for higher maniraptorans.

Comparison of *Microraptor* to *Bambiraptor feinbergi* (Burnham et al., 2000) is to be expected, since *Bambiraptor* is among the smallest of the dromaeosaurids and has been described as being very birdlike. *Bambiraptor* was not included in our phylogenetic analysis because only a preliminary description of the specimen has been published; likewise, a comparison of *Bambiraptor* and *Microraptor* will be postponed until further information on *Bambiraptor* is made available.

#### PHYLOGENETIC ANALYSIS

To evaluate the systematic position of *Microraptor* we scored it for characters based on the Theropod Working Group Matrix<sup>5</sup> (see appendix 2). The matrix contains 208 characters, 13 of which are ordered. Two kinds of analyses were done. The first analysis (fig. 31) used composite coding for *Microraptor* based on the three available specimens (IVPP V12330, CAGS 20-8-001, CAGS 20-7-004). The second included all three *Microraptor* specimens, each one coded individually. All of Xu et al.'s (2000) codings were accepted for the holotype specimen, except those for characters 83 and 145. Upon inspection of the holotype, we decided that Xu et al.'s (2000) codings could not be verified and that the state of the two characters could not be determined from the available material.

All phylogenetic analyses were performed in NONA ver. 1.9 (Goloboff, 1993) through the WinClada ver. 0.9.99b (Nixon, 1999) interface. For both the first and second analyses, a heuristic search implementing 1000 replicates of the Tree Bisection and Re-grafting (TBR) algorithm was performed. The 10 shortest trees from each replicate were retained, and then additional TBR branch-swapping was performed among the shortest

<sup>5</sup> This matrix is matrix 2002.2 of the Theropod Working Group. This matrix, character descriptions, and explanation are available at <http://research.amnh.org/vertpaleo/norell.html>

of the retained trees. *Allosaurus fragilis* and *Sinraptor dongi* were chosen as outgroups, and all branches with a minimum length of zero were collapsed.

The first analysis, using composite coding for *Microraptor*, recovered 240 equally most parsimonious trees of 600 steps; 457 of the 1000 replicates (45.7%) recovered trees of 600 steps, indicating a fairly good recovery of the shortest trees. The second analysis, with each of the three *Microraptor* specimens coded individually, produced almost identical results. The second search found 240 equally most parsimonious trees of 600 steps; 380 of the 1000 replicates (38.0%) found trees of 600 steps. Strict consensus of the most parsimonious trees from each analysis yielded trees of identical topology, except that in the second analysis the three *Microraptor* specimens formed a monophyletic group as the sister taxon to other dromaeosaurids. The strict consensus tree of 600 steps from the first (composite) analysis (fig. 31), which has a CI of 0.43 and an RI of 0.71, is the one that will be discussed below.

Our results corroborate the general hypotheses of theropod relationships proposed by Gauthier (1986) in that a monophyletic Deinonychosauria composed of monophyletic troodontid and dromaeosaurid groups forms the sister group to Avialae. The Deinonychosauria clade is supported by several characters, including a reduced or absent pterygoid flange, a splenial that is widely exposed on the lateral surface of the mandible, and a distinct groove or ridge near the lateral edge along the distal end of the deltopectoral crest. This node has a Bremer support of 1. This result is also congruent with that of Xu et al. (2000), in that *Microraptor* is the most basal dromaeosaurid.

Other parts of this phylogeny are, for the most part, congruent with recent phylogenetic analyses (Norell et al., 2001; Xu et al., 2002). The tree is identical to that obtained in Norell et al. (2001) except for the placement of the Avialae, Dromaeosauridae, and Troodontidae clades. This result is slightly more resolved than the one yielded by Xu et al. (2002), especially in the case of oviraptorosaurs. The inclusion of *Microraptor* in the Theropod Working Group Matrix causes the asymmetrical foot (character 208) to be

lost as a troodontid synapomorphy, since *Microraptor*, like troodontids, has a slender metatarsal II and a robust metatarsal IV.

This phylogeny has important implications for avialan origins. Because both *Sinovenator* and *Microraptor*, the most basal taxa of their respective clades (in addition the dromaeosaurid *Sinornithosaurus*), are small animals, small size optimizes as primitive for the Deinonychosauria, as suggested by Xu et al. (2002). Looking at *Archaeopteryx*, small size is obviously also primitive for Avialae. While we do not view this as support for any model of flight origin (i.e., trees down vs. ground up), it does nullify complaints such as that of Feduccia and Wild, who stated that “even the most birdlike theropods were relatively large, have shortened forelimbs, were terrestrial cursors, and never ventured up trees” (Feduccia and Wild, 1993: 565–566).

The discovery of *Microraptor* and other Jehol theropods has had important implications for understanding coelurosaur phylogeny and the evolution of Avialae. Certainly the discovery and description of other new specimens will shed even more light on these questions.

## CONCLUSIONS

1. The position of *Microraptor* as the sister taxon to other dromaeosaurs is corroborated.
2. A monophyletic Deinonychosauria that is the sister taxon to Avialae is corroborated.
3. Small size is primitive at the node of Deinonychosauria + Avialae (Paraves).
4. Including *Microraptor* in the Theropod Working Group Matrix results in the loss of a pes with a slender, laterally compressed metatarsal II and a robust metatarsal IV as a troodontid apomorphy.

## ACKNOWLEDGMENTS

We thank the Chinese Academy of Geological Sciences and the National Geological Museum of China for the loan of the two *Microraptor* specimens. We are grateful to Xu Xing and the Institute for Vertebrate Paleontology and Paleoanthropology for access to the *Microraptor* holotype. The figures were meticulously prepared by Mick Ellison.

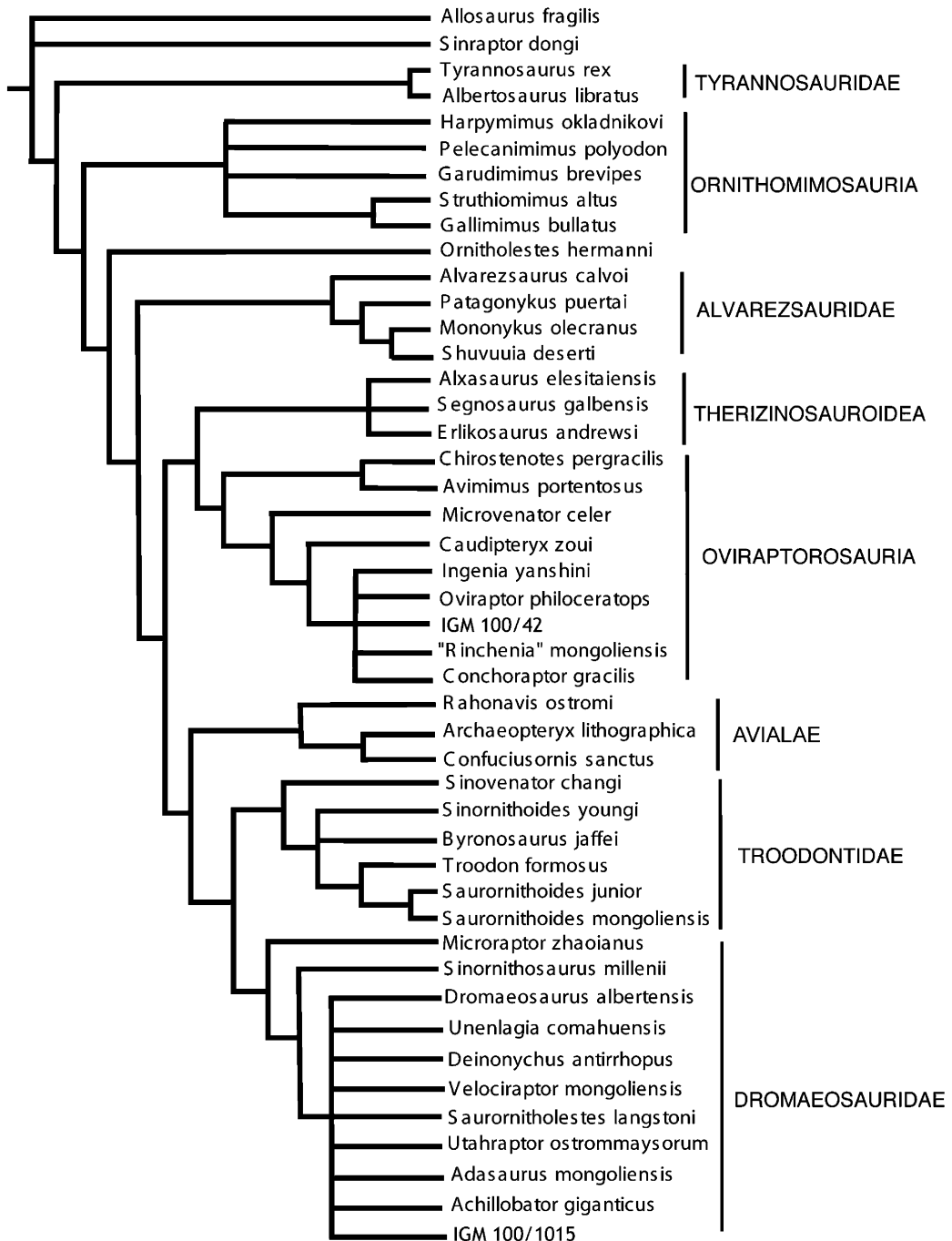


Fig. 31. Strict consensus of 240 most parsimonious trees from analysis using composite coding for *Microraptor*. Tree length = 600 steps, CI = 0.43, RI = 0.71.



This project was supported by the Division of Paleontology at the American Museum of Natural History, Vivian Pan, and Lynette, Richard, and Byron Jaffe. Discussions with Diego Pol and Peter Makovicky and the comments of Thomas Holtz improved the quality of this paper.

#### REFERENCES

- Britt, B.B., P.J. Makovicky, J. Gauthier, and N. Bonde. 1998. Postcranial pneumatization in *Archaeopteryx*. *Nature* 395: 374–376.
- Burnham, D.A., K.L. Derstler, P.J. Currie, R.T. Bakker, Z.-H. Zhou, and J.H. Ostrom. 2000. Remarkable new birdlike dinosaur (Theropoda: Maniraptora) from the Upper Cretaceous of Montana. *University of Kansas Paleontological Contributions New Series* 13: 1–14.
- Chiappe, L.M., S.-A. Ji, Q. Ji, and M.A. Norell. 1999. Anatomy and systematics of the Confuciusornithidae (Theropoda: Aves) from the Late Mesozoic of Northeastern China. *Bulletin of the American Museum of Natural History* 242: 1–89.
- Clark, J.M., M.A. Norell, and R. Barsbold. 2001. Two new oviraptorids (Theropoda: Oviraptorosauria), Upper Cretaceous Djadokhta Formation, Ukhaa Tolgod, Mongolia. *Journal of Vertebrate Paleontology* 21: 209–213.
- Clark, J.M., M.A. Norell, and L.M. Chiappe. 1999. An oviraptorid skeleton from the Late Cretaceous of Ukhaa Tolgod, Mongolia, preserved in an avianlike brooding position over an oviraptorid nest. *American Museum Novitates* 3265: 1–36.
- Currie, P.J. 1987. Bird-like characteristics of the jaws and teeth of troodontid theropods (Dinosauria, Saurischia). *Journal of Vertebrate Paleontology* 7: 72–81.
- Currie, P.J. 1995. New information on the anatomy and relationships of *Dromaeosaurus albertensis* (Dinosauria: Theropoda). *Journal of Vertebrate Paleontology* 15: 576–591.
- Feduccia, A., and R. Wild. 1993. Birdlike characters in the Triassic archosaur *Megalanosaurus*. *Naturwissenschaften* 80: 564–566.
- Forster, C.A., S.D. Sampson, L.M. Chiappe, and D.W. Krause. 1998. The theropod ancestry of birds; new evidence from the Late Cretaceous of Madagascar. *Science* 279: 1915–1919.
- Gauthier, J. 1986. Saurischian monophyly and the origin of birds. *In* K. Padian (editor), *The origin of birds and the evolution of flight*. *California Academy of Science Memoirs* 8: 1–55.
- Goloboff, P.A. 1993. NONA version 1.9 [computer program]. S. M. de Tucumán, Argentina: published by the author.
- Hutchinson, J.R. 2001. The evolution of pelvic osteology and soft tissues on the line to extant birds (Neornithes). *Zoological Journal of the Linnean Society* 131: 123–168.
- Ji, Q., M.A. Norell, K.-Q. Gao, S.-A. Ji, and D. Ren. 2001. The distribution of integumentary structures in a feathered dinosaur. *Nature* 410: 1084–1088.
- Kielan-Jaworowska, A., and R. Barsbold. 1972. Narrative of the Polish-Mongolian paleontological expeditions 1967–1971. *Palaeontologia Polonica* 27: 5–13.
- Makovicky, P.J. 1995. Phylogenetic aspects of the vertebral morphology of Coelurosauria (Dinosauria, Theropoda). Thesis, University of Copenhagen.
- Makovicky, P.J. 1997. Postcranial axial skeleton, comparative anatomy. *In* P. J. Currie and K. Padian (editors), *Encyclopedia of dinosaurs*: 579–590. San Diego, CA: Academic Press.
- Makovicky, P.J., and P.J. Currie. 1998. The presence of a furcula in tyrannosaurid theropods, and its phylogenetic and functional implications. *Journal of Vertebrate Paleontology* 18: 143–149.
- Middleton, K.M. 1999. Morphological basis for hallucal orientation in fossil birds. *Journal of Vertebrate Paleontology* 19(Suppl.): 64A.
- Nixon, K.C. 1999. WinClada version 0.9.99 (beta) [computer program]. Ithaca, NY: published by the author.
- Norell, M.A., and P.J. Makovicky. 1997. Important features of the dromaeosaur skeleton: information from a new specimen. *American Museum Novitates* 3215: 1–28.
- Norell, M.A., and P.J. Makovicky. 1999. Important features of the dromaeosaur skeleton II: information from newly collected specimens of *Velociraptor mongoliensis*. *American Museum Novitates* 3282: 1–45.
- Norell, M.A., and P.J. Makovicky. In press. Dromaeosauridae. *In* D.B. Weishampel, P. Dodson, and H. Osmólska (editors), *The Dinosauria*, 2nd ed. Berkeley, CA: University of California Press.
- Norell, M.A., J.M. Clark, and P.J. Makovicky. 2001. Phylogenetic relationships among coelurosaurian theropods. *In* J. Gauthier and L. F. Gall (editors), *New perspectives on the origin and early evolution of birds: proceedings of the International Symposium in Honor of John H. Ostrom*. New Haven, CT: Peabody Museum of Natural History Yale University.
- Novas, F.E., and P.F. Puerta. 1997. New evidence concerning avian origins from the Late Cretaceous of Patagonia. *Nature* 387: 390–392.
- Osmólska, H., and R. Barsbold. 1990. Troodontidae. *In* D. B. Weishampel, P. Dodson, and H.

- Osmólska (editors), *The Dinosauria*: 259–268. Berkeley: University of California Press.
- Ostrom, J.H. 1969. Osteology of *Deinonychus antirrhopus*, an unusual theropod from the Lower Cretaceous of Montana. Peabody Museum of Natural History Yale University Bulletin 30: 1–165.
- Paul, G. 1988. *Predatory dinosaurs of the world*. New York: New York Academy of Sciences.
- Sereno, P. 1999. The evolution of dinosaurs. *Science* 284: 2137–2147.
- Unwin, D.M., A. Perle, and C. Trueman. 1995. *Protoceratops* and *Velociraptor* preserved in association: evidence for predatory behavior in dromaeosaurid dinosaurs. *Journal of Vertebrate Paleontology* 15(Suppl. to 3): 57A–58A.
- Wellnhofer, P. 1974. Das fünfte Skelettexemplar von *Archaeopteryx*. *Palaeontographica Abteilung A Palaeozoologie-Stratigraphie* 147: 169–216.
- Wellnhofer, P. 1992. A new specimen of *Archaeopteryx* from the Solnhofen limestone. In K.E. Campbell, Jr. (editor), *Papers in avian paleontology honoring Pierce Brodkorb*. Natural History Museum of Los Angeles County Science Series 36: 3–24.
- Wellnhofer, P. 1993. Das siebte Exemplar von *Archaeopteryx* aus den Solnhofener Schichten. *Archaeopteryx* 11: 1–48.
- Xu, X., M.A. Norell, X.-L. Wang, P.J. Makovicky, and X.-C. Wu. 2002. A basal troodontid from the Early Cretaceous of China. *Nature* 415: 780–784.
- Xu, X., X.-L. Wang, and X.-C. Wu. 1999. A dromaeosaurid dinosaur with a filamentous integument from the Yixian Formation of China. *Nature* 401: 262–266.
- Xu, X., Z.-H. Zhou, and X.-L. Wang. 2000. The smallest known non-avian theropod dinosaur. *Nature* 408: 705–708.

APPENDIX 1  
MEASUREMENTS OF *MICRORAPTOR ZHAOIANUS* (IN MILLIMETERS)

		CAGS 20-7-004									
		Right					Left				
<b>SKULL</b>											
<b>Dentary</b>											
	Anteroposterior length					33.36					25.10
	Rostral dorsoventral height					7.18					x
	Caudal dorsoventral height					3.61					3.50
	Tooth row length					24.88*					x
<hr/>											
		Maximum length of centrum		Maximum height of centrum		Maximum width across transverse processes		Height of neural spine		Length of neural spine	
		CAGS	CAGS	CAGS	CAGS	CAGS	CAGS	CAGS	CAGS	CAGS	CAGS
		20-7-004	20-8-001	20-7-004	20-8-001	20-7-004	20-8-001	20-7-004	20-8-001	20-7-004	20-8-001
<hr/>											
<b>VERTEBRAE</b>											
<b>Cervicals</b>											
	8(?)	x	3.51			x	6.42				
	9(?)	6.07	4.18			9.89	6.59				
<b>Dorsals</b>											
	1	5.97	x	x	x	9.23		x	x	x	x
	2	x	x	5.68	x	x		4.24	x	x	x
	3	7.40	x	x	x	11.09		x	3.54	x	4.25
	4	6.54	>4.32	x	3.52*	8.12		x	x	x	>4.11
	5	7.10	6.38	x	3.83	7.74		x	x	x	x
	6	5.39	6.34	x	4.10	9.13		x	3.65	x	4.31
	7	5.18	6.40	x	4.19	9.80		x	3.52	x	4.79
	8	6.14	6.42	4.32	4.00	x		3.34	3.84	5.01	4.52
	9	5.76	6.45	4.52	3.97	x		3.20	3.83	4.19	>3.97
	10	5.97	6.34	4.33	3.98	x		3.60	>3.45	4.44	4.28
	11	6.08	6.32	3.86	4.16	x		3.30	3.99	3.88	4.28*
	12	6.10	6.24	4.08	4.17	x		3.48	3.76	4.07	4.21
	13	6.12	6.12	3.58	3.96	x		x	3.47*	x	4.01*
<b>Sacrals</b>											
	5(?)		5.28								11.74*
	6(?)		4.91								15.10*
<b>Caudals</b>											
	1	6.19	4.25			11.47	10.58*				
	2	7.52	5.28			10.54	14.14*				
	3	8.58	5.63			x	12.39				
	4	13.12	6.16			x	10.64*				
	5	16.54	7.42			x	11.98*				
	6	19.42	10.32			x	8.52*				
	7	18.49	14.70			x	x				
	8	17.90	18.47			x	x				
	9	17.16	18.91			x	x				
	10	17.24	18.45			x	x				
	11	16.82	18.80			x	x				
	12	17.30	>17.51			x	x				
	13	17.17	>10.71			x	x				
	14	16.38	17.64			x	x				
	15	15.94	18.08			x	x				

APPENDIX 1  
(continued)

	Maximum length of centrum		Maximum width across transverse processes	
	CAGS 20-7-004	CAGS 20-8-001	CAGS 20-7-004	CAGS 20-8-001
16	16.36	16.96	x	x
17	15.48	17.08	x	x
18	14.06	16.74	x	x
19	13.79	16.90	x	x
20	12.55	16.06*	x	x
21	11.22	15.82	x	x
22	10.64	15.67*	x	x
23	9.03	14.00*	x	x
24	7.44	11.49	x	x
25	7.62	10.66*	x	x
26	5.58	9.46	x	x

	CAGS 20-7-004		CAGS 20-8-001	
	Right	Left	Right	Left
<b>PECTORAL GIRDLE</b>				
Scapula				
Anteroposterior length			>27.07	43.01
Coracoid				
Length of dorsal margin			>13.56	16.04
Sternum				
Anteroposterior length			38.39	37.99*
Minimum mediolateral width			11.98	11.48
Mediolateral width across xiphoid process			14.00	13.93
<b>FORELIMB</b>				
Humerus				
Length (proximodistal)	62.06	61.25	62.88	>46.05
Maximum width across deltopectoral crest	x	9.74	11.30	x
Proximal anteroposterior depth	x	6.34	6.28	6.38
Distal transverse width	8.73	x	x	x
Distal anteroposterior depth	x	5.96	7.46	6.21
Least diameter of shaft	4.72	4.99	5.35	4.95
Ulna				
Length (proximodistal)	>51.64	53.78	53.50*	>40.67
Proximal anteroposterior depth	x	5.20	6.99	6.35
Distal anteroposterior depth	6.47	6.20	x	x
Least diameter of shaft	4.02	4.05	3.83	3.96
Radius				
Length (proximodistal)	x	48.01*	x	48.30*
Proximal anteroposterior depth	x	x	x	4.28
Distal anteroposterior depth	x	3.49	x	4.34*
Least diameter of shaft	x	2.39*	2.37	2.18

APPENDIX 1  
(continued)

	CAGS 20-7-004		CAGS 20-8-001	
	Right	Left	Right	Left
<b>MANUS</b>				
<b>METACARPALS</b>				
<b>Metacarpal I</b>				
Length (proximodistal)	x	7.84		
Proximal transverse width	x	3.76		
Distal transverse width	x	2.92		
<b>Metacarpal II</b>				
Length (proximodistal)	>31.27	>27.26		
Proximal transverse width	3.09	3.00		
<b>Metacarpal III</b>				
Length (proximodistal)	>29.79	>25.28		
Proximal transverse width	2.04	1.94		
<b>PHALANGES</b>				
<b>I-1</b>				
Length (proximodistal)	x	20.45		
Proximal transverse width	x	2.18		
Distal transverse width	x	2.67		
<b>I-2</b>				
Length along outer curve	x	x	14.40	
Height of facet	x	x	2.69	
Height at flexor tubercle	x	x	5.38	
<b>II-1</b>				
Length (proximodistal)	13.26	x		
Proximal transverse width	3.54	x		
Distal transverse width	2.73*	3.20		
<b>II-2</b>				
Length (proximodistal)	16.39	15.88		
Proximal transverse width	3.40	3.39		
Distal transverse width	2.31*	2.29*		
<b>II-3</b>				
Length along outer curve	10.26	9.49	10.27	
Height of facet	1.74	1.80*	1.86	
Height at flexor tubercle	4.06	3.88	4.09	
<b>III-1</b>				
Length (proximodistal)	10.12	x		
Proximal anteroposterior depth	1.93	x		
Distal anteroposterior depth	2.01	x		
<b>III-2</b>				
Length (proximodistal)	4.10	x		
Proximal anteroposterior depth	1.81	x		
Distal anteroposterior depth	1.63	x		
<b>III-3</b>				
Length (proximodistal)	10.37	10.06		
Proximal anteroposterior depth	1.88	1.69		
Distal anteroposterior depth	1.22	1.18		

APPENDIX 1  
(continued)

	CAGS 20-7-004		CAGS 20-8-001	
	Right	Left	Right	Left
<b>PELVIC GIRDLE</b>				
<b>Ilium</b>				
Length (proximodistal)	x	x	40.04	40.81
Length anterior to acetabulum	x	x	16.64	17.47
Length posterior to acetabulum	x	x	14.91	14.36
Height above acetabulum	x	x	6.87	7.11
<b>Pubis</b>				
Length (proximodistal)	52.39*	52.73	52.77	x
Transverse width of distal symphysis		4.62	5.92	
Maximum transverse width of pubic apron		6.74*	9.48*	
<b>Ischium</b>				
Length (proximodistal)	25.22	25.06	26.84	26.20
Anteroposterior proximal length	x	x	10.68	10.02*
Anteroposterior length across obturator process (distal anteroposterior length)	8.16	8.26*	10.78	10.95*
Distance from apex of posterior process to iliac process	17.16*	16.60	17.12	17.32
<b>HINDLIMB</b>				
<b>Femur</b>				
Length	74.75	74.26	74.77	74.40
Proximal transverse width	8.46	8.92	x	x
Proximal anteroposterior depth	x	x	7.96	7.75
Distal transverse width	x	8.56	x	x
Distal anteroposterior depth	7.92	x	4.94	x
Least diameter of shaft	4.27	4.38	5.12	4.87
<b>Tibiotarsus</b>				
Length	>77.64	94.22	95.51*	94.14
Maximum proximal transverse width	7.54	6.51	>5.98	9.46
Maximum distal transverse width	x	6.54	x	6.83
Least diameter of shaft	5.60	5.40	4.42	5.38
Length of ascending process of astragalus	x	x	x	9.37
<b>Fibula</b>				
Length	>74.85	85.67*	x	87.2
Proximal anteroposterior depth	2.20	2.10	x	2.58
Distal anteroposterior depth	x	0.43	x	0.42
<b>PES</b>				
<b>METATARSALS</b>				
<b>Metatarsal I</b>				
Length	x	x	8.09	x
Distal anteroposterior depth	x	x	0.98	x
<b>Metatarsal II</b>				
Length	x	44.51	x	45.89
Proximal transverse width	x	2.05	x	x
Proximal anteroposterior depth	x	x	x	3.72
Distal transverse width	x	2.47	2.48	x
Distal anteroposterior depth	x	x	2.69	2.78

APPENDIX 1  
(continued)

	CAGS 20-7-004		CAGS 20-8-001	
	Right	Left	Right	Left
<b>Metatarsal III</b>				
Length	x	47.76	x	49.39
Proximal transverse width	x	1.20?	x	x
Distal transverse width	x	2.29	2.40	3.15
Distal anteroposterior depth	x	x	2.56	x
<b>Metatarsal IV</b>				
Length	x	46.80	x	48.50*
Proximal transverse width	x	2.96?	x	x
Proximal anteroposterior depth	x	x	x	>2.55
Distal transverse width	x	2.91	x	x
<b>Metatarsal V</b>				
Length	x	22.03	x	23.98
Proximal transverse width	x	0.78	x	x
Proximal anteroposterior depth	x	x	x	0.58
Distal transverse width	x	0.68	x	x
Distal anteroposterior depth	x	x	x	0.91
<b>PHALANGES</b>				
<b>I-1</b>				
Length	x	x	5.35	5.26
Proximal transverse width	x	x	x	2.20
Proximal anteroposterior depth	x	x	1.46	x
Distal anteroposterior depth	x	x	1.42	x
<b>I-2</b>				
Length along outer curve	x	x	3.34	x
Proximal anteroposterior height	x	x	1.79*	x
Height of facet	x	x	1.46	x
<b>II-1</b>				
Length	x	6.88	6.91	7.38
Proximal transverse width	x	x	3.00	x
Proximal anteroposterior depth	x	2.36	2.37	3.23
Distal transverse width	x	x	2.89	x
Distal anteroposterior depth	2.44	2.42	2.38	2.75
<b>II-2</b>				
Length	6.77	7.24	7.59	x
Proximal anteroposterior depth	2.64	2.80	4.33	4.05
Distal anteroposterior depth	2.65	2.75	3.23	x
<b>II-3</b>				
Length	12.88	13.24	16.04	15.20*
Proximal anteroposterior height	4.12	4.47	5.27*	x
Height of facet	2.35	2.53	3.93	x
<b>III-1</b>				
Length	x	9.95	9.74	10.05
Proximal transverse width	x	2.10	2.41	2.44
Distal transverse width	x	2.20	2.31	2.16
Distal anteroposterior depth	x	x	x	2.62
<b>III-2</b>				
Length	x	7.74	8.20	8.24*
Proximal transverse width	x	2.29	2.63	x
Proximal anteroposterior depth	x	x	x	2.59
Distal transverse width	x	1.64	2.29	x

APPENDIX 1  
(continued)

	CAGS 20-7-004		CAGS 20-8-001	
	Right	Left	Right	Left
III-3				
Length	x	6.13	8.10	7.88
Proximal transverse width	x	1.58	x	x
Proximal anteroposterior depth	x	x	2.84	2.83
Distal transverse width	x	1.54	x	x
Distal anteroposterior depth	x	x	2.29	2.26
III-4				
Length along outer curve	x	9.39	9.37	9.51
Proximal anteroposterior height	x	3.40	3.54	3.71
Height of facet	x	2.04	2.59	2.91
IV-1				
Length	x	7.30	8.39	8.14
Proximal transverse width	x	2.89	2.03*	x
Proximal anteroposterior depth	x	x	x	2.58*
Distal transverse width	x	2.40*	2.18	x
Distal anteroposterior depth	x	x	x	2.77
IV-2				
Length	x	5.40	5.97	5.72
Proximal transverse width	x	2.06*	1.80	x
Proximal anteroposterior depth	x	x	x	2.20*
Distal transverse width	x	2.42	1.89	x
IV-3				
Length	x	5.01	4.16	4.37*
Proximal transverse width	x	2.11	1.75	x
Distal transverse width	1.73	2.62	1.77	x
IV-4				
Length	5.01	5.42	5.90	5.66
Proximal anteroposterior depth	2.09	1.98	2.32	2.01
Distal anteroposterior depth	1.73	2.12	2.03	2.08
IV-5				
Length along outer curve	8.95	9.18	9.02	x
Proximal anteroposterior height	2.86	2.96	3.60*	x
Height of facet	1.85	1.68	2.07	x

Measurements marked with an \* are estimated values; x indicates that no measurement is available.





APPENDIX 2  
(continued)

		1
	5555555556666666666777777777788888888888999999999999	
	12345678901234567890123456789012345678901234567890	
<i>Allosaurus fragilis</i>	000010000000000101?0100100000001001000000000001000	
<i>Ingenia yanshini</i>	120100?011111-----?---????????????????????1??01-??2?	
" <i>Rinchenia</i> " <i>mongoliensis</i>	120100??11111-----????????????????????0?????21	
<i>Oviraptor philoceratops</i>	120100?01?11-----????????????????????0???????	
<i>Conchoraptor gracilis</i>	1201?0?011111-----?????????010?1?013110??1????	
IGM 100/42	1201001011111-----101110110010111001?201-?0021	
<i>Chirostenotes pergracilis</i> <sup>a</sup>	120000?01??1-----????????1101?1????112??0?????	
<i>Dromaeosaurus albertensis</i>	0000111100000001011001?????????????????????????????	
<i>Deinonychus antirrhopus</i>	0?0011?100001101011000?110001100?111011??0011011?	
<i>Velociraptor mongoliensis</i>	0000111?00001101011000011?001100111101111000110111	
<i>Mononykus olecranus</i>	????????????22?--00?????????1?1?1110001????10?2???	
<i>Shuuvuia deserti</i>	0100002100?0222--0000?011111101110?0??12010120122	
<i>Patagonykus puertai</i>	??11??????10?2???	
<i>Alvarezsaurus calvoi</i>	????????????????????????????????????100??????2?10?2?12?	
<i>Ornitholestes hermanni</i>	0000?0?00000??01011001?????011?01010000?000?0010?	
<i>Microvenator celer</i>	?20????????????????????????011?0?1100011100??0?1-1002?	
<i>Archeopteryx lithographica</i>	000000??0000220--000100?1?1??00?0?0?0?0?00110122	
<i>Avimimus portentosus</i>	1?000??0111?-----?0110101101010?00?100???????	
<i>Caudipteryx zoui</i>	120????????01-----00?????0?00?????????0?01-?????	
<i>Unenlagia comahuensis</i>	??111?11????0???????	
<i>Confuciusornis sanctus</i>	010010?00011??-????????0????????????10??02??0???????	
<i>Rahonavis ostromi</i>	????????????????????????????????????01?11????101?011122	
<i>Struthiomimus altus</i>	010010200011-----001?101100001000011000000001	
<i>Gallimimus bullatus</i>	000000200011-----0011101100001000011000000001	
<i>Garudimimus brevipes</i>	0?????02?0?11-----?????????????????0??1?0???????	
<i>Pelecanimimus polyodon</i>	0?00????????00222--00001?????????????????????????????	
<i>Harpymimus okladnikov</i>	??0????????220--11-?????????????????????????????????	
<i>Troodon formosus</i>	??1?????????01110100100??111110010101111000?1020?	
<i>Saurornithoides mongoliensis</i>	0?10?1????0011101001?????????1??0?0?0??100??1????	
<i>Byronosaurus jaffei</i>	001?11????00221--001?0?0?????????01010?????????0?02??	
<i>Saurornithoides junior</i>	0?1??1????001110100100????????????????????11000?1020?	
<i>Sinornithoides youngi</i>	??10?????001110?001?????11?001?????????0011?101	
<i>Segnosaurus galbinensis</i>	???000?000?001000001????????????????????????0???????	
<i>Erlikosaurus andrewsi</i>	00000200010001000001-?????????????????????????????????	
<i>Akasaurus elesitaiensis</i>	0?0?????????????10?0001?????????????0?01000001?001??02?	
<i>Tyrannosaurus rex</i>	00001001000000010110110100000-0000110000010000?001	
<i>Albertosaurus libratus</i>	00001001000000010110110100000-?0001100000100000001	
<i>Sinraptor dongi</i>	000010?0000000010110100100000001001000000000000????	
<i>Adasaurus mongoliensis</i>	????????????00??	
<i>Utahraptor ostrommaysorum</i>	????????????0????1011?1?????????????1?????????0?0?011?	
<i>Saurornitholestes langstoni</i>	????????????1101011?00?110001100111101101100?1011?	
<i>Achillobator giganticus</i>	????????????00001011?????0?01100?1110?????????0?011?	
IGM 100/1015	0000111100001101011000?????0?1???????????????????????	
<i>Sinornithosaurus milleni</i>	?000?1????00110?1100?????????1?1?1?????0?00?1?1?1?	
<i>Sinovenator changii</i>	0?1?????000011110?1?????11?1010001010?01000110221	
<i>Microaptor zhaioianus</i>	??0?1????0011000000?????001?1??01?000?0??0110?11	

<sup>a</sup>Including *Caenaganthus*.





## APPENDIX 3

## ANATOMICAL ABBREVIATIONS USED IN FIGURES

a	astragalus	ls	last sacral vertebra
aa	ascending process of astragalus	lsc	left scapula
ac	acromion	lsp	left sternal plate
act	accessory crest	lt	lesser trochanter
ais	antiliac shelf	lu	left ulna
b	bifurcation of anterior extension of chevron	lxp	lateral xiphoid process
c	caudal vertebra	mc	metacarpal
ca	calcaneum	mco	medial condyle
ce	cervical vertebra	mt	metatarsal
cf	cuppediticus fossa	ns	neural spine
ch	chevron	ns1	neural spine lamina
chf	chevron facet	ol	olecranon process
cn	cnemial crest	op	obturator process
cp	carotid process	pa	pubic apron
cs	claw sheath	pb	pubic boot
d	dorsal vertebra	ph	phalanx
dp	deltapectoral crest	pis	posterior process of ischium
dr	dorsal rib	pnf	pneumatic foramen
dt	dorsal tubercle of ilium	pp	parapophysis
ech	anterior extension of chevrons	ppd	pubic peduncle
ep	epipophysis	ppr	pubic process of ischium
epz	anterior extension of prezygapophyses	prz	prezygapophysis
f	furcula	pz	postzygapophysis
fc	fibular crest	pt	posterior trochanter
fi	fibula	rc	right coracoid
g	gastralia	rf	right femur
gl	glenoid	rh	right humerus
gt	greater trochanter	ri	right ilium
h	head of femur	ris	right ischium
ift	iliofibularis tubercle	rp	right pubis
ip	iliac process of ischium	rra	right radius
isp	ischadic peduncle	rsc	right scapula
it	internal tuberosity	rsp	right sternal plate
lc	left coracoid	ru	right ulna
lco	lateral condyle	sc	semilunate carpal
lig	ligament pit	sr	sternal rib
lp	left pubis	srf	sternal rib attachment facet
lr	lateral ridge	t	distal tarsal
lra	left radius	ti	tibia
		tp	transverse process
		tu	tubercle